Experiments 30a and 30b

INTERACTION OF GAMMA RAYS WITH MATTER

INTERACTION OF GAMMA RAYS WITH MATTER

INTRODUCTION: NUCLEAR DECAY AND GAMMA RAY PRODUCTION

Many of the experiments in Physics 7 study radioactive decay processes in atomic nuclei and the interaction of nuclear emissions with matter. In experiments 30a and 30b we will learn how to use a scintillation detector (a powerful tool for the study of the spectra of high-energy photons) and will become familiar with commonly-observed nuclear decay processes. Experiment 30a is a required experiment for Physics 7 and is a prerequisite for many of the other experiments; it will be the first experiment you perform. Experiment 30b continues the investigation of the interaction of gamma rays with matter and may be completed later in the term.

Nucleons, nuclear states, and nuclear forces

An atom's nucleus is a bound state of several *nucleons* — protons and neutrons — each of which has a *rest energy* of approximately 0.94 GeV, over 1800 times that of an electron.[1] The total number of nucleons in a nucleus is called its *atomic mass* (or *atomic weight*) and will be denoted by the symbol *A*. The number of protons in a nucleus is called the nucleus's *atomic number* and is denoted by the symbol *Z*. Protons are observed to have an electric charge which cancels that of an electron to at least 21 decimal places, whereas neutrons are observed to carry a net electric charge of no more than 10^{-21} that of the proton.[2] The total electric charge of a nucleus is thus equal to *Ze*, with the SI value of *e* defined (in 2019) to be exactly $1.602176634\times10^{-19}$ coulombs. Nuclei with the same *Z* but different *A* are called *isotopes* and are denoted as in the following examples:

$$^{133}\mathrm{Cs} \qquad ^{137}\mathrm{Cs} \qquad ^{137}\mathrm{Ba}$$

The element (cesium or barium in the above examples) corresponds to the proton number *Z*; the total number of nucleons *A* is given by a numeric superscript prefix. Occasionally the atomic number is included as a subscript, as in $^{57}_{26}\mathrm{Fe}$.

Historical notes: the electron was discovered by J. J. Thompson at Cambridge, UK, in 1897; the nucleus by Ernest Rutherford, Hans Geiger, and Ernest Marsden in 1911 at the University of Manchester, UK. Thompson then went on to discover the existence of different nuclear isotopes

---

[1] Energies will be expressed in *electron volts* (eV, 1.6×10^{-19} joule), with keV = 10^3 eV, MeV = 10^6 eV, GeV = 10^9 eV, etc. A particle's mass will be stated as its *rest energy*: mc^2, where *m* is the particle's *rest mass*. Although in the text we may talk of a particle's mass, we will really mean its rest energy (in eV).

[2] The cancellation of the proton and electron charges is currently assumed to be *exact* in the SI system of measurement and in nearly all acceptable theories of fundamental physics, although this is actually a most nontrivial statement about the world. Charge is also considered to be a *Lorentz invariant*, so that it has the same value in all reference frames. Modern experimental tests of the charge neutrality of bulk matter were reviewed by *Unnikrishnan and Gillies*, http://dx.doi.org/10.1088/0026-1394/41/5/S03.

(of neon) in 1913. Not to be outdone, Rutherford discovered (and named) the proton in 1917. By 1929, research on nuclear spin at Caltech (by Franco Rasetti) had demonstrated that theories of the nucleus were incomplete, and in 1932 James Chadwick discovered the neutron at Cambridge. Nucleons are *fermions*, each with spin ½, and as such obey *Pauli exclusion* among the states occupied by identical particles (proton-proton or neutron-neutron), analogous to the arrangement of an atom's electrons.

Recall that atomic electrons (also fermions) are found to occupy any of several different energy levels and orbitals. The lowest energy configuration of an atom's electrons is its *ground state*, and other configurations result in excited atomic states. Excited atomic states will eventually transition ("decay") in one or more steps to the atom's ground state, usually by the emission of photons. The allowable energy levels of the atom's outermost electrons ("valence" electrons) are typically separated by energies of a few eV (give or take an order of magnitude). Because $hc = 1240\,\text{eV nm}$, transitions among these states involve near infrared to ultraviolet photons (1000's of nm to 100nm wavelengths). On the other hand, the inner shell electrons of all but the lightest atoms are much more strongly bound, resulting in transition energies of 10^3–10^5 eV (1 to 100's of keV). Photons in this energy range are called *x-rays*.

Nuclear structure is analogous to but much more complicated than this atomic electron structure: nucleons are arranged in various levels to determine a nuclear state. Excited nuclear states can also decay by the emission of photons (among other processes). Because an atomic nucleus is so much smaller than an atom ($\sim 10^{-5}$Å vs. $\sim$1Å), quantum kinematics (i.e. the uncertainty principle) demand that such transitions will often involve much higher energies than do atomic transitions, typically 10's to 1000's of keV. Photons emitted during nuclear transitions are termed *gamma rays* or *γ-rays*. Named by Rutherford, nuclear γ radiation was discovered by Paul Villard in 1900 in Paris. Unfortunately, "γ-ray" is often used to refer to any high-energy photon (energy above 100 keV or so), regardless of its origin. In Physics 7 we will be more specific, however, and consider γ-ray photons to be produced only by a nuclear transition, so that, for example, an 87 keV photon produced by a lead atom electron transition is an *x*-ray, whereas a 14 keV photon produced by a nuclear transition in ^{57}Fe is a γ-ray, even though it has a lower energy.

The nucleons themselves are actually composite particles each composed of 3 *quarks*. The quarks are bound together by the *strong force* (or *color force*), which is a couple of orders of magnitude greater than the Coulomb force within a nucleon (distances $\lesssim 1\text{fm} = 10^{-5}$Å, also called a *fermi*). The 3-quark nucleons, which are *color-neutral*, can then bind together to form a nucleus by a much-weakened remnant of the strong field, analogous to the *van der Waals* Coulomb force which can very weakly bind electrically-neutral noble gas atoms together. This inter-nucleon force is termed the "nuclear force" or "residual strong force," and it falls off exponentially with distance, becoming negligible at ranges beyond a few fermi. The first reasonably successful theory of the nuclear force was formulated by Hideki Yukawa in 1935 at Osaka University, Japan, but a useful theory of the strong force and the internal structure of nucleons had to wait for the 1970's. That theory, *quantum chromodynamics*, has a "strong"

connection to Caltech: the contributions of Murray Gell-Mann, Richard Feynman, and David Politzer immediately come to mind.

Uncertainty principle considerations suggest that each nucleon, when confined to the nuclear volume with radius ~1 fermi, must have a kinetic energy of ~10–20 MeV and a speed of ~0.2 *c*. Additionally, the repulsive Coulomb force between two close-packed protons adds a potential energy of another 12 MeV (6 MeV per proton).[3] Clearly, the force between nucleons must result in an attractive potential large enough to more than balance these energies and generate the observed nuclear bound states — energies a million times greater than the 13.6 eV binding energy of the hydrogen atom.

The attractive nuclear force between a pair of bound nucleons is approximately independent of whether either one is a proton or neutron but is strongly dependent on their separation and the orientation of their spins (inherent angular momenta). The proton-neutron pair of the small deuterium nucleus ("deuteron"), for example, has a net nuclear binding energy of 1.1 MeV per nucleon, showing that the nuclear force between them results in an attractive potential energy about 10% greater than their kinetic energies. Replacing the deuteron's proton with a neutron in this case, however, keeps them from binding together: Pauli exclusion and quantum kinematics of the two identical neutrons prevent them from finding a state compact enough for the nuclear force to bind them. Two protons would fare even worse because of their added electrostatic repulsion. Add a proton to a neutron pair or a neutron to a proton pair, however, and a strong net nuclear attraction is the result — ${}^{3}_{1}\mathrm{H}$ (tritium) in its ground state has a binding energy of 2.8 MeV/nucleon, and ${}^{3}_{2}\mathrm{He}$ is a stable isotope with a net binding energy of 2.6 MeV per nucleon. Add yet another nucleon, and ${}^{4}_{2}\mathrm{He}$ achieves an especially strong total nuclear force, resulting in a binding energy of over 7 MeV/nucleon. This value turns out to approach those of the heavier naturally-occurring isotopes: 7 to 9 MeV/nucleon (except lithium).

Beta decay

One more fundamental force of nature is important for our understanding of the nucleus: the *weak force*, which is responsible for the great majority of natural radioactive decay processes. The weak force is the only known interaction which can change the nature of an elementary particle — it can change an electron into a neutrino (and vice versa) or a quark into one of a different type (called "flavor"). The archetypal change mediated by the weak interaction is the spontaneous decay of a free (isolated) neutron into a proton, electron, and *antineutrino* — a decay whose *half-life* (median lifetime) is a little over 10 minutes. Within a nucleus the weak interaction can also convert a proton to a neutron, either by (1) utilizing an inner-shell atomic electron, converting it into a neutrino, or (2) creating a *positron* (the electron's antiparticle) and a neutrino. In all cases, of course, the daughter products' total rest energy must be no more than

[3] See the first 30a Prelab problem for how to calculate these estimates.

that of the parent so that the process is energetically favorable (in the case of the free neutron, the difference is only about 0.08%). Each of these processes is a form of *beta decay*, named after the emitted *β-radiation* (electrons or positrons) investigated by Rutherford and Henri Becquerel circa 1899–1900. Because beta decay is by far the most common process which modifies the nucleus, and it does not change the nucleus atomic weight *A*, nuclei with the same *A* can usually be considered as different states of essentially the same underlying system. The nucleus resulting from beta decay is often left in an excited state; when it decays to its ground state *γ*-ray photons are usually emitted. These beta decay processes and the relevant nuclear energy levels for the several radioactive *γ*-ray emitters we have in the lab are illustrated by the diagrams in this document's *APPENDIX A: Nuclear beta decay diagrams*.

Consider this relatively simple example of such a process: the decay of $^{60}_{27}\mathrm{Co}$ to $^{60}_{28}\mathrm{Ni}$ described by the decay diagram shown in Figure 1. The process begins with the beta decay of a neutron in the cobalt nucleus. The weak interaction converts one of the neutron's two *down quarks* into an *up quark*, changing that nucleon into a proton. That interaction also creates an *electron* and a companion *antineutrino* which together carry away both the energy (mass) difference and the electric charge difference between the original cobalt nucleus and that of the daughter nickel nucleus. This step is indicated in the diagram by the "β^-" diagonal arrow. The "*Q*" value of this step indicates the maximum kinetic energy which the outgoing electron (the "beta particle") could carry. Usually the electron will have a significantly lower kinetic energy, the remainder being carried away by the antineutrino (which, by the way, is not electrically charged).

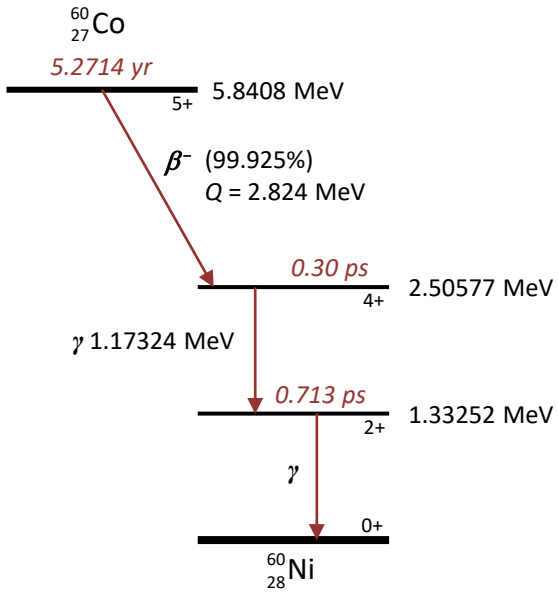

Figure 1: The radioactive decay of Cobalt 60.

The resulting nickel-60 nucleus has not yet reached its ground state, however. It does so in two steps, each resulting in a photon emission (*γ*-ray). Each intermediate-state half-life is indicated in Figure 1 (both are a fraction of a picosecond) as well as the emitted photon energies (1.17324 and 1.33252 MeV). Also indicated in the diagram are each state's angular momentum and parity quantum numbers (5+, 4+, etc.).

The half-life of the cobalt-60 beta decay is 5.2714 years. In this time, on average, half of a population of cobalt-60 nuclei will have undergone beta decay to become nickel-60; each successive period of 5.2714 years reduces the remaining population by another fact of 2.

SCATTERING AND ABSORPTION OF HIGH-ENERGY PHOTONS BY MATTER

In these experiments you will study high-energy photons by observing the reaction products as the photons interact with a solid material object: your detector. The detector you will use for this experiment is a *scintillator* attached to a *photomultiplier* tube. The two scintillator materials you will use are sodium iodide (NaI) and, in Experiment 30b, an acrylic plastic ($C_5O_2H_8$). As we will discuss, these detectors work by converting energy from a high-energy photon into a flash of visible light which is detected by the photomultiplier.

The γ-ray photons we will use will typically have energies on the order of 1MeV. Their wavelengths are much smaller than the size of an atom:

$$\lambda = hc/E \sim 12.4 \text{ KeV Å}/10^6\text{eV} \approx 10^{-2}\text{ Å}$$

As a result, such a γ-ray photon does not see a solid material as a continuous medium or even a collection of atoms; it sees even the densest of materials as a vacuum containing hard particles: mostly electrons with the occasional nucleus. We can analyze the interaction of a high-energy photon with matter as a succession of interactions with individual electrons or nuclei. The exception to this general rule is an inner electron of a heavy atom, which can interact with a high-energy photon as a resonant absorber rather than as a simple particle. The radius of an inner electron orbit in an atom with atomic number Z is approximately $0.5\text{Å}/Z$, and its binding energy is roughly $Z^2 \times 14\text{eV}$, so for $Z \geq 30$ these inner electron orbits have compact sizes and have energies approaching the lower end of the γ-ray photon range.

Because of these considerations, the two main processes by which γ-rays interact with matter are *Compton scattering* and *photoelectric absorption* (for energies up to 1 or 2MeV). A third process, *pair production*, occurs if the photon has an energy greater than twice the electron rest energy (~1MeV), and this becomes the dominant process above around 10MeV (this also depends strongly on the Z of the target atoms). In what follows we will discuss these three processes in more detail. Most of this discussion assumes some familiarity with the relativistic kinematics described in detail in the Ph7 website's general appendix Relativistic Kinematics. Refer to the appendix Cross Sections for the definitions of the differential and total cross section.

These symbols will be used in the following sections:

k_0 , k	incident and scattered photon energies $(hc/\lambda = \hbar\omega)$ or momenta
m_e	electron rest energy $= 0.511$ MeV (i.e. taking $c \equiv 1$; $m_e c^2 \to m_e$)
r_e	classical electron radius $= e^2/(4\pi\varepsilon_0 m_e) = 2.82\times10^{-5}$ Å
σ_e	Thompson (classical) electron cross section $= (8\pi/3) r_e^2 = 6.65\times10^{-25}\text{cm}^2$
α	fine structure constant $= e^2/(4\pi\varepsilon_0 \hbar c) \approx 1/137$

Compton scattering

Compton scattering is the elastic scattering (or collision) of a high-energy photon with a single charged particle (an electron in our case) as shown in Figure 1. The energy of the outgoing photon scattered by a free electron is given by equation (30.1) (see General Appendix A, pp A-10 to A-11).

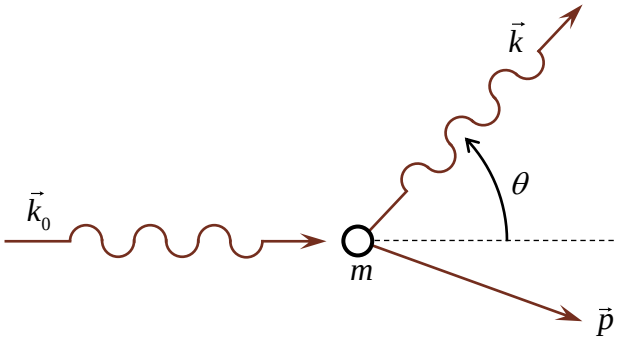

Figure 2: Compton scattering of a photon by an initially stationary particle. This figure is from Relativistic Kinematics.

Compton scattering formula

$$k = \frac{k_0}{1+\frac{k_0}{m}(1-\cos\theta)} \quad \text{or, equivalently,} \quad \frac{1}{k} = \frac{1}{k_0} + \frac{1}{m}(1-\cos\theta) \tag{30.1}$$

The outgoing electron kinetic energy following a Compton scattering event is $T_e = k_0 - k$. Because the photon and electron rest masses differ, the incoming photon cannot transfer all of its kinetic energy to the target electron, even in a direct (head-on) collision (unlike the case of a pair of colliding billiard balls). The maximum energy transferable to the electron is called the *Compton edge energy* (T_{edge}) and is derivable from equation (30.1) when $\theta = 180°$:

Compton edge energy

$$T_{edge} = \frac{k_0}{1+\frac{m}{2k_0}} \tag{30.2}$$

The differential cross section to scatter the photon by angle θ is given by the *Klein-Nishina* cross section, equation (30.3), first derived jointly by Oskar Klein and Yoshio Nishina in 1929. Integrating this formula over solid angle Ω results in the total cross section plotted in Figure 2.

$$\frac{d\sigma}{d\Omega} = \frac{r_e^2}{2}\left(\frac{k}{k_0}\right)^2\left(\frac{k}{k_0}+\frac{k_0}{k}-\sin^2\theta\right) \tag{30.3}$$

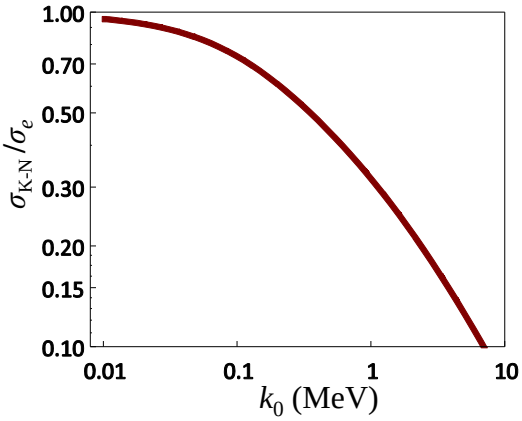

Figure 3: The integrated, total Klein-Nishina cross section for Compton scattering as a function of the incoming photon energy (see (30.3)). The total cross section is scaled by the *Thompson scattering electron cross section*, σ_e. In the low energy limit the cross section approaches this classical value given by *Thompson scattering theory*, presented in Appendix B of the Experiment 32 notes Compton Scattering.

Photoelectric absorption

Photons cannot be absorbed by single electrons in the process:

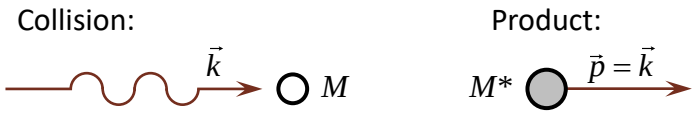

This absorption cannot conserve both momentum and energy unless $M^* > M$ (see Relativistic Kinematics, pp A-7 to A-8). Since an electron is an elementary particle, its rest energy cannot change, and this condition cannot be satisfied. A *composite* object such as an atom or nucleus, however, has internal degrees freedom which can absorb the extra energy of the collision, so that $M^* > M$, and both momentum and energy can be conserved. In the case of a high-energy photon, photoelectric absorption by an atom results in the ejection of an atomic electron from the atom. The combined energies and momenta of the escaping electron and the recoil of the ionized atom provide for energy and momentum conservation in the process. Usually an inner electron is ejected by this process, and the atom (now a positive ion) emits several ultraviolet (UV) and *x*-ray photons as its remaining electrons cascade downward to fill the atom's vacated electron state (this emission process is known as *fluorescence*). Figure 3 shows this process.

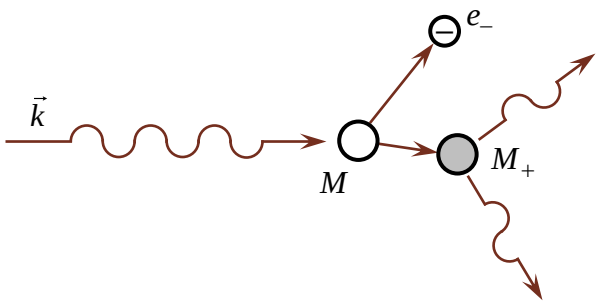

Figure 4: Photoelectric absorption of a high-energy photon is a resonant process involving one of the innermost electrons in a heavy atom. The electron is ejected from the atom; subsequent transitions of less tightly bound electrons result in the emission of UV and *x*-ray photons. The total momenta and kinetic energies of the ejected electron and recoiling ion match that of the incoming photon, so its absorption is kinematically allowed.

The absorption of the photon by an atom is, in a sense, a *resonant process* (analogous to the driven harmonic oscillator of Physics 6, Experiment 2) with a characteristic frequency associated with the binding energy E_{bind} of the atomic electron: $\omega = E_{\text{bind}}/\hbar$. For γ-ray photons it is the innermost electrons (the *K*-shell) which have binding energies closest to the photon energy, so these electrons are most likely to be involved (as long as $E_{\text{bind}} < k_0$). Because of this resonant behavior and the fact that transfer of momentum to the nucleus is required, this process has a very strong Z dependence, typically $\propto Z^5$, and a very strong dependence on the γ-ray energy, approximately $\propto k_0^{-3}$ as it approaches E_{bind} for a particular electron shell from higher energies. As k_0 decreases through E_{bind} there is an abrupt decrease in the photoelectric cross section (called an *absorption edge*), since the photon now doesn't have sufficient energy to ionize that particular electron. Each electron shell (*K*, *L*, *M*, etc.) in the atom has an absorption edge associated with its E_{bind}. For k_0 well above the *K*-edge energy of an atom but well less than $m_e c^2$, *Leo*[4] section 2.7.1 gives equation (30.3) as an approximate expression for the photoelectric absorption cross section.

$$\sigma_{photo} \approx \sigma_e 4\sqrt{2}\,\alpha^4 Z^5 \left(\frac{m_e c^2}{k_0}\right)^{7/2} \tag{30.4}$$

Pair production (*Experiment 32b*)

The process of pair production involves the conversion of a high-energy photon into an electron-positron (particle-antiparticle) pair (see Figure 5). As with photoelectric absorption, however, this process cannot occur in empty space because momentum conservation is violated: the outgoing particle pair has a total momentum rest-frame, but a lone, incoming photon does not. Thus we need a nearby nucleus to provide a third particle which can be used to conserve

[4] Leo, *Techniques for Nuclear and Particle Physics Experiments* (2nd revised ed., Springer-Verlag: 1987, 1994). The lab library has several copies. We refer to this text as *Leo*.

momentum. This momentum transfer is accomplished through the Coulomb interaction between the outgoing pair and the nucleus, so the cross section for pair production turns out to be $\propto Z^2$ (*Leo* 2.7.3). Of course, we must have the incoming photon energy $k_0 > 2m_e c^2 \approx 1\,\text{MeV}$ or pair production is precluded by energy conservation (see General Appendix A for a more careful derivation of the threshold energy). As k_0 increases above the threshold, the cross section for pair production increases dramatically. Photons with energies exceeding 100MeV can produce heavier particle-antiparticle pairs.

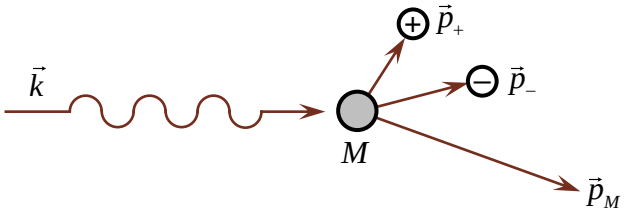

Figure 5: Pair production by a high-energy photon interaction with an atomic nucleus *M*. If the incoming photon energy is great enough, the photon may decay into a particle-antiparticle pair.

In a solid object such as a scintillator, the positron produced in such an interaction will eventually lose its kinetic energy through collisions with atomic electrons. It will then bond with an electron of the solid, and the pair will quickly annihilate, creating two or more high-energy photons. Interestingly, both the electron-positron pair production and annihilation processes are intimately associated with photon-electron Compton scattering — the modern, highly-successful theory of *quantum electrodynamics* demonstrates that at a deep, fundamental level, these three interactions are manifestations of a single, fundamental process describing the interaction of charged particles with electromagnetic fields.

THE APPARATUS: A SCINTILLATION GAMMA RAY SPECTROMETER

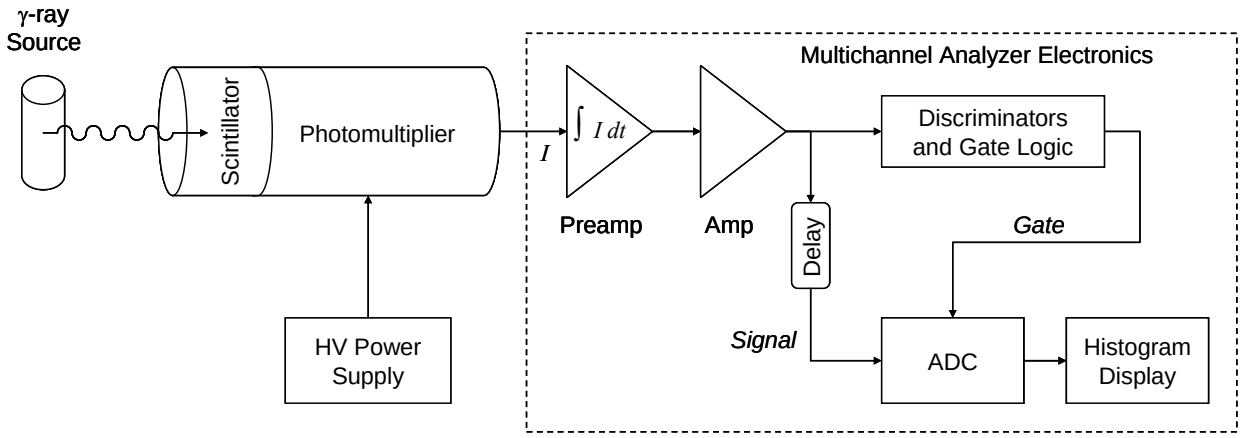

Figure 6: A scintillation gamma ray spectrometer system. The scintillator and photomultiplier are optically coupled and shielded from external light sources. Often the high-voltage power supply and the multichannel analyzer electronics are integrated into a single unit with a computer control and data display interface.

The setup you will use for experiments 30a and 30b is outlined in Figure 6, a block diagram of a typical high-energy photon spectrometer system. It uses a scintillation detector feeding a *Multichannel Analyzer* (MCA) being used in its *pulse height analysis* mode.

Detection of the high-energy photon takes place when the photon interacts with an atom in the scintillator through one of the processes discussed previously and transfers some or all of its energy to one or two electrons (and, possibly, a positron). These high-speed, charged particles quickly and efficiently lose their kinetic energy through collisions with other electrons in the scintillator in a cascading reaction (involving UV and even *x*-ray generation as atomic electrons fall into lower levels once occupied by electrons knocked out of many atoms). Very quickly, the initial energy deposited by the high-energy photon is distributed among many thermalized electrons and their parent ions. The initial electron's kinetic energy has been converted into the total binding energy of these electron-ion pairs.[5]

The scintillator material is designed so that as the electron-ion pairs recombine, many visible-light photons are generated. These photons are directed toward the attached photomultiplier tube, which converts this flash of light (due to the recombination energy release) into a pulse of current. In a well-designed scintillator the number of these visible-light photons will be proportional to the energy deposited by the original, high-energy photon's interactions. The total charge transferred by the current pulse output from the photomultiplier should thus also be proportional to the deposited energy, so a spectrum of energy deposited by a high-energy photon

[5] These slow-moving electrons occupy the lower states in the scintillator material's *conduction band*. The missing electrons from the parent atoms form *holes* in the material's *valence band*. The *energy gap* between the conduction and valence bands represents the binding energies of the ion's missing electrons.

source may be constructed by the system electronics. Let's examine the parts of the apparatus:

Source: A small amount of γ-ray emitter sealed in a plastic rod. For these experiments the emitter activity is in the *μCurie* range ($\sim 10^4$ *Becquerel*, or decays/sec).

Scintillator: A transparent, solid crystal or piece of acrylic plastic material designed so that a high-energy photon interacting with the atoms in the material will deposit energy which is efficiently converted into a flash of visible light. The lab has two different scintillator materials:

Sodium iodide crystal (NaI): The light output is a pulse with a decaying exponential tail, $I = I_0 \exp(-t/\tau)$, with time constant τ of about 0.25μs.

Plastic scintillator: These scintillators are much faster than NaI, with all of the light coming out in a very short burst. The photomultiplier current output width is a few nanoseconds and it is most often determined by the photomultiplier and not the plastic scintillator.

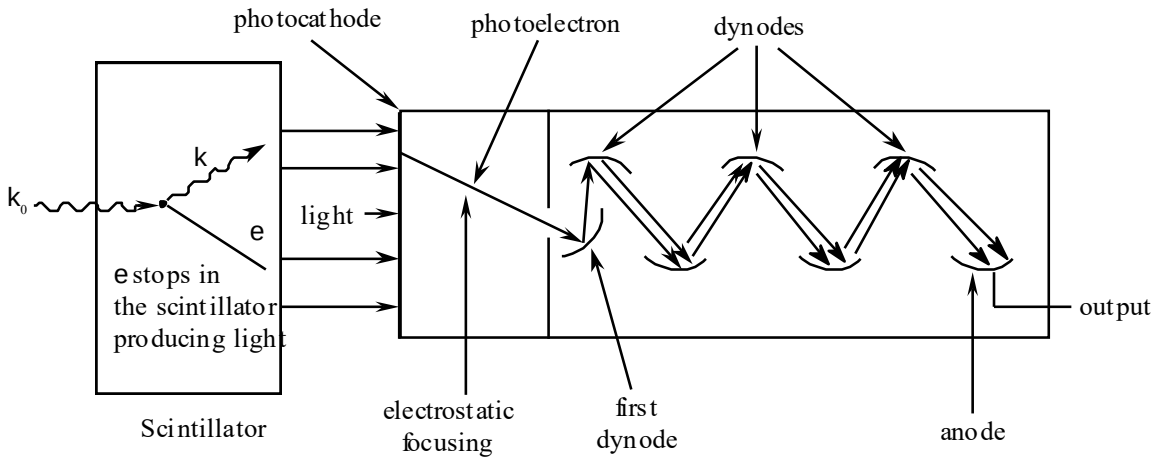

Figure 7: A photomultiplier tube attached to a scintillator. The potential difference between successive dynodes in the tube accelerates an electron so that when it strikes the next dynode it can knock out two or more electrons, and they are then accelerated toward the subsequent dynode. Depending on the voltage applied to the tube, the final anode may receive from 10^4 to 10^7 electrons for each electron emitted by the photocathode.

Photomultiplier: Figure 7 shows a sketch of a scintillator coupled to a photomultiplier tube. The photomultiplier's main parts and their purpose are the following:

Photocathode: This is a very thin film that converts, through the photoelectric effect, some of the incident optical photons into electrons (the efficiency for conversion is around 15%). These photoelectrons are accelerated and focused into a small opening just in front of the first dynode.

Dynodes: These do the actual electron multiplication. When an electron with kinetic energy of the order of 200 eV strikes a dynode, around three electrons are ejected by the impact.

These secondary electrons are again accelerated and subsequently strike the following dynode. The gain of a photomultiplier is then given by $g = g_0{}^n$, where g_0 is the gain per dynode and *n* the number of dynodes. For the devices that you will use $g_0 \approx 3$ and $n = 10$, therefore $g \approx 10^5$. The gain g_0 is a strong function of the high voltage applied to the photomultiplier, so you will adjust the high voltage applied across the dynode array to set the desired photomultiplier gain.

Anode: This final surface collects all the electrons from the last dynode and routes them to the photomultiplier output in the form of a pulse of current.

High Voltage (HV) Power Supply: The photomultiplier tube requires a high voltage (on the order of 1000 volts) for proper operation. Since the photomultiplier gain is a sensitive function of the high voltage, this supply must be well-regulated for the system to have stable gain. The Experiment 30 setups have a HV power supply which is integrated with the MCA electronics and is controllable using the MCA software. Other experiments have detectors powered by a separate, external HV supply. The voltage in this case must be adjusted using the controls on the HV supply itself.

Preamplifier and Filter/Amplifier: The output from the photomultiplier is a pulse of current. The total charge in the current pulse is proportional to the number of electrons ejected by the photocathode, which is determined by the energy deposited in the scintillator by the incoming photon. The current pulse is amplified and integrated by a *current integrating preamplifier*, followed by a high-gain *filter/amplifier* whose output is a voltage pulse with peak amplitude proportional to the integrated charge from the photomultiplier. The preamplifier works by using the photomultiplier current pulse to charge a small capacitor; the voltage across the capacitor is proportional to the charge stored in it. The NaI scintillator + photomultiplier output charges the capacitor in a microsecond or less. The resulting tiny capacitor voltage is greatly amplified by the preamplifier. That output is then further amplified and shaped by the filter/amplifier into a narrow voltage pulse (width of a couple of microseconds, height up to a few volts) corresponding to a detector event.

Note that if more than photomultiplier pulse is generated by multiple detection events during this pulse integration and shaping time, the total charge output by the photomultiplier will be interpreted by the electronics to be a single, large pulse.

The filter/amplifier's gain is set by the experimenter as the product of two factors: its *coarse gain*, settable to one of several selectable values, and its *fine gain*, continuously adjustable through a range of about a factor of 2 or 3. The gain adjustment for this experiment is controlled using the MCA software.

Several experiments are set up so that the output of the filter/amplifier is monitored by an oscilloscope so you can see the actual voltage pulses being processed by the MCA. This is an important troubleshooting tool which can greatly aid you in determining whether the system is working properly and will help you set the proper photomultiplier voltage and amplifier gain. The scope should be set to around 1 volt/division and 1 μsec/division.

ADC: The *analog-to-digital converter* (ADC) samples, measures, and digitizes the peak voltage of a pulse arriving from the filter/amplifier whenever it receives a gate signal from the discriminator (described below). The ADC output is a *channel* (or *bin*) *number* corresponding to the digitized voltage of the pulse. The channel number can range from 0 (for a tiny pulse) to 1024 or higher (for a large pulse). The *conversion gain* is set using the MCA software and determines the total number of channels output by the ADC (1024 is a typical setting). By using more channels, you get higher resolution but fewer events/channel for a fixed total number of events.

Discriminators and Gate Logic: Lots of low-level noise is present in the output of the photomultiplier and preamplifier, and we don't want the ADC to waste time digitizing it. A small preset threshold must be exceeded before the MCA interprets the input as a valid signal pulse. In addition, there are the user-controllable *lower level discriminator* (LLD) and *upper level discriminator* (ULD). These two adjustments set a window within the full-scale output voltage range of the amplifier. The discriminator and gate logic circuitry then generate an output gate signal whenever a pulse from the amplifier exceeds the preset threshold and has an amplitude which falls within the window set by the LLD and ULD. The output pulse then signals the ADC to measure and catalog the amplifier output as described above. The delay circuit shown in Figure 6 makes sure the gate pulse gets to the ADC before the signal does.

The ADC is a precise, highly linear device which can take a microsecond or more to perform a conversion. During this conversion time, the ADC cannot respond to another pulse, so there is a ***dead time*** associated with the conversion. The ***live time*** is that fraction of time the ADC spends waiting for a new pulse to arrive (i.e., not busy performing a conversion). You want the live time to be a large fraction of the total time you spend collecting data (the ***real time***). This unwanted dead time fraction is why the LLD and ULD are important.

If an uninteresting signal with a very high pulse rate is present in the detector output, the ADC could spend most of its time measuring this uninteresting signal and will quite likely miss pulses you are interested in. Properly setting the LLD and ULD will allow the ADC to ignore these unwanted pulses, because no gate signal is generated for them.

INTERPRETING THE MCA HISTOGRAM DISPLAY

A typical MCA spectrum

Together the MCA electronics and the computer (using the MCA software) generate a histogram of number of events recorded for each digitized pulse height (ADC channel number). Using the MCA software you may save a histogram data set, clear the display and then start a new measurement. During the measurement the scintillator output pulses are amplified and processed by the MCA, building a new histogram display as the measurement proceeds. You may stop the measurement at any time so that you can study the histogram and process it using several tools available in the MCA software. Figure 8 shows a typical histogram display (for a ^{137}Cs source). Each channel along the *x*-axis corresponds to a pulse-height interval or *bin* (ADC channel number); the *y*-axis displays how many pulses were received within that bin.

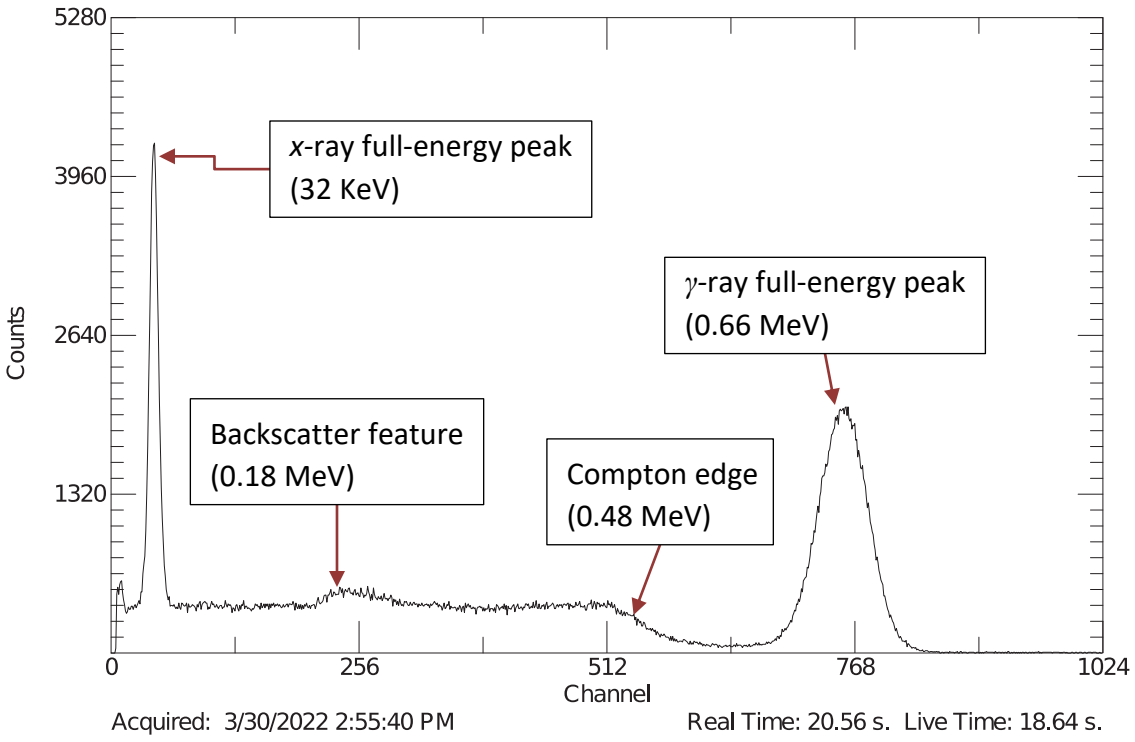

Figure 8: Typical MCA histogram display for ^{137}Cs, using a sodium iodide scintillator. Several important features are annotated. These features are explored in the next few sections of the text. The *x*-axis is the ADC channel number (bin), and the *y*-axis is the number of events recorded within that ADC bin number. Calibration of the instrument using known-energy sources will allow the experimenter to convert ADC bin number to energy deposited in the scintillator. This spectrum was obtained with *ORTEC*® digiBASE and MAESTRO® products used in Experiment 30a.

Detector electrons and transferred energy

One must carefully consider the expected characteristic signatures of the three basic interaction processes (Compton scattering, photoelectric absorption, and pair production) in order to

successfully interpret an MCA spectrum of a high-energy photon source. As already mentioned, a rapid sequence of events within the scintillator generates a visible-light flash which is converted to a current pulse and processed by the MCA electronics to produce a resulting increment in a particular histogram channel. In this section we discuss this sequence in more detail for each of the three basic interactions in the scintillator.

First examine the Cesium-137 decay diagram shown on the first page of *Appendix A: Nuclear beta decay diagrams*. The decay process can result in the emission of high-energy photons with two different energies: either a 0.66 MeV gamma-ray or a 32 keV x-ray (resulting from a conversion electron event). The most important thing to remember about how the MCA system responds to an interaction of one of these photons with atoms in the detector is that:

The MCA displays a spectrum of the *kinetic energies of individual electrons* ejected from atoms in the detector by γ-ray photons—*not the energies of the photons themselves*.

This fact is particularly relevant to the displayed spectrum resulting from Compton scattering of photons in the scintillator, but first we consider photoelectric absorption by an atom.

Photoelectric absorption and the full-energy peak

In this process the incident high-energy photon is absorbed by an atom of the scintillator, transferring all of its energy to a single inner atomic electron (usually a 1s electron), leaving a vacant electron state in the atom. As this electron escapes from its parent atom, its initial kinetic energy is reduced by the state's binding energy as it climbs out of the atom's Coulomb potential well. At the same time, the remaining electrons in the parent atom quickly cascade down into lower energy states, generating UV and *x*-ray photons which are then absorbed by other atoms in the scintillator, generating additional high energy electrons and photons.

These ejected electrons will each have a large initial kinetic energy, but this energy is quickly shared among many hundreds or thousands of weakly-bound valence electrons in the scintillator material through an avalanche of collisions, a process analogous to the collisions of balls on a billiards table or collisions among the molecules of a gas. Thus the incident photon's energy is efficiently and completely converted through this process into the combined binding energies of many valence electron-ion pairs (a completely negligible amount of energy is also transferred due to recoils of the various atoms, which is then lost as heat). The subsequent recombination of these electron-ion pairs generates the visible-light photons collected by the photomultiplier, as described previously.

Photoelectric absorption therefore results in the capture of all of the photon's energy by the detector, and therefore each photoelectric absorption interaction deposits the energy of the incident photon. The resulting MCA spectrum has a clear peak at the channel corresponding to this energy. These *full-energy peaks* provide two prominent features in the ^{137}Cs spectrum shown in Figure 8: one for the 0.66 MeV γ-ray photons and one for the 32 keV *x*-ray photons.

Compton scattering and the Compton edge

In this process an incident γ-ray photon gives up some fraction of its initial energy k_0 to some weakly-bound, valence electron in the scintillator (which comprise the vast majority of the electrons in any material). Depending on the angle of the collision (Figure 2), the outgoing photon carries away energy k (equation (30.1)). If the outgoing photon subsequently escapes from the scintillator, then that photon's energy k will not be detected. The valence electron involved in the scattering process leaves the atom with kinetic energy $T_e = k_0 - k,$ which is then transferred to a large number of electron-ion pairs as described above.

The MCA energy spectrum produced by many independent Compton scattering events with various scattering angles is therefore continuous from $T_e = 0$ (corresponding to $\theta = 0^o$ in equation (30.1)) up to the incident photons' *Compton edge* energy T_{edge}, corresponding to $\theta = 180^o$ and given by equation (30.2). This Compton contribution to the MCA spectrum is readily apparent in Figure 8 as the broad area with ~400 counts/channel in the left half of that spectrum. All were produced by Compton scatters of the 0.66 MeV γ-ray photons emitted by the ^{137}Cs source. The actual shape of the Compton spectrum is strongly dependent on the composition and size of the scintillator and the energy resolution of the MCA system, as addressed below. These factors are explored in more detail in the procedure for Experiment 30b.

The Compton edge energy T_{edge} generally happens to be located very close to the channel position corresponding to 2/3 of the height of the scintillator Compton spectrum at its high-energy end (about channel 512 in Figure 8), as described in this document's *Appendix C: MCA spectrum energy resolution* and illustrated in Figure 13 on page 30–C–6.

Multiple interactions

If the scintillator crystal is large and dense enough, then the outgoing photon from a Compton scattering event may experience another interaction within the scintillator before it can escape. Traveling at the speed of light, these multiple events happen in a fraction of a nanosecond, much shorter than the time resolution of the detector system (~μsec for NaI). Each successive photon interaction deposits energy in the scintillator in the form of additional ionized atoms as already described, and because multiple interactions take place in such a short time, the total deposited energy is processed by the detector system and displayed in the MCA histogram as a single event.

A rapid succession of Compton scattering events generated by a single incoming photon can transfer more energy to the scintillator than could a single Compton event. Thus, multiple Compton scatters can transfer a total energy greater than the Compton edge energy, T_{edge}. The signature of such successive Compton events is evident in the increased counts recorded in the energy gap between the Compton edge energy at 0.48 MeV and the full-energy peak at 0.66 MeV in the MCA display in Figure 8.

The energy of the outgoing photon following a large-angle Compton scattering event is often much lower than that of the incident photon. Since the probability of a photoelectric absorption increases rapidly as the photon energy decreases (see equation (30.4) and this document's *Appendix B: Mass attenuation coefficient charts*), the final interaction in a multiple event chain is usually photoelectric absorption of the final, low-energy photon. In this case the total energy transferred to the scintillator by the entire sequence of events is equal to the original, incoming photon's energy k_0, and the combined event sequence results in a detector output which contributes to the photon full-energy peak. In fact, a sequence of multiple interactions culminating in photoelectric absorption is the most probable route to full-energy detection of high-energy γ-rays, since the probability of photoelectric absorption by the scintillator is usually much smaller than that for Compton scattering. This document's *Appendix B: Mass attenuation coefficient charts* provides the details.

The larger the scintillator volume, the more likely it is that multiple interactions will occur. The higher the *Z* of the atoms in the scintillator, the more likely it is that photoelectric absorption will occur.

Thus a large NaI scintillator (iodine *Z* = 53) can have a much more prominent full-energy peak than can a smaller scintillator, especially if it made of low-*Z* atoms such as silicon or an acrylic.

Also note that because outgoing photon energies are smallest for Compton scatters near 180°, events that would have been near the Compton edge in the displayed MCA spectrum are more likely to be part of a sequence of multiple events culminating in photoelectric absorption (and contribute to the full energy peak) than are Compton events depositing smaller energies. This effect explains why the Compton area of the NaI spectrum shown in Figure 8 has a much less prominent "hump" near the Compton edge than does a spectrum produced by a plastic scintillator or does the calculated spectrum shown in Figure 13 on page 30–C–4.

Backscatter feature

The source's γ-ray photons can Compton scatter off of anything, not just the material in the scintillator. If such a photon scatters by an angle near 180° somewhere outside, but nearby, the scintillator, the outgoing photon may then enter the scintillator. If so, it arrives with an energy near the difference between the full energy peak and Compton edge energies: $k_0 - T_{edge}$. Photoelectric absorption of such photons within the scintillator may produce a continuum of small peaks in the MCA spectrum as shown in Figure 8 (shaped like a small reflection of the original γ-ray's Compton spectrum near T_{edge}).

Pair production and escape peaks (Experiment 30b)

In Figure 9 we revisit Figure 5, but we neglect the tiny energy transferred to the nucleus, and we add the eventual particle-antiparticle annihilation of the positron with some electron in the material. The total kinetic energy of this photon-generated electron-positron pair is $T_+ + T_- = k_0 - 2m_e$, the original photon's energy minus the combined rest energies of the two freshly-created particles. Both the electron and the positron carom around through the scintillator until each stops, eventually depositing all of their combined kinetic energy in the form of electron-ion pairs.

The positron, however, has a positive charge, and after a very short time it forms an "atom" with one of the many electrons in the material: this electron-positron bound state is called *positronium* (like a hydrogen atom but with a positron instead of a proton). In around 10^{-10}sec the electron and the positron *annihilate*, creating two photons. Since the positronium atom was essentially at rest in the scintillator, the two photons are emitted with equal energies and in opposite directions in order to conserve linear momentum. There is also a finite but small possibility that the positron may be annihilated while in flight, or that the eventual positronium annihilation emits *three* photons; we ignore these possibilities because: (1) in a solid material they rarely occur, and (2) the annihilation photons they produce can have a wide range of energies.

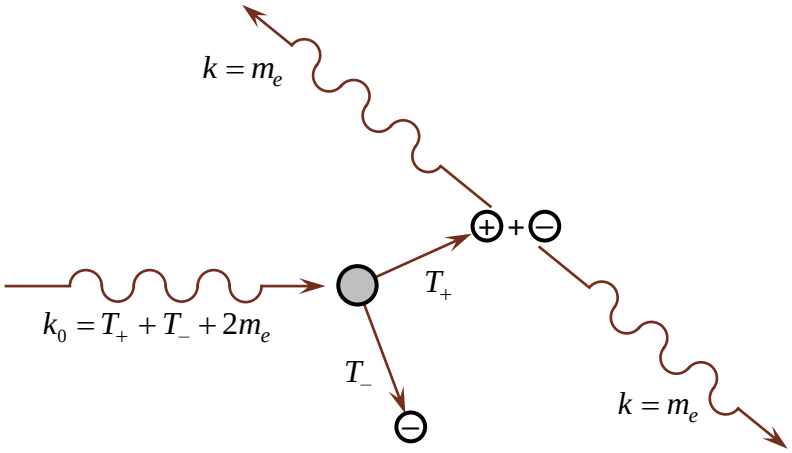

Figure 9: Pair production by an incoming photon and subsequent annihilation of the outgoing positron with some electron in the scintillator. The positron first loses its kinetic energy (T_+) by ionizing many atoms in the material, as does the high-speed electron of the pair (energy T_-). One or both of the photons produced by the eventual electron-positron annihilation may interact with the scintillator, capturing some of its energy, or they may both escape without further interaction. Note that each annihilation photon has energy k equal to the rest energy of an electron.

There are then three cases of note to consider depending on what happens to the *annihilation photons* (all three cases contribute to the ^{232}Th spectrum shown in Figure 10 on page 19):

Full-energy peak: If both electron-positron annihilation photons are absorbed by the scintillator through photoelectric absorption before they can escape, the total energy deposited by all processes is equal to the total energy of the incoming γ-ray, k_0, thus contributing to the full-energy peak.

One-escape peak: If only one of the electron-positron annihilation photons is photoelectrically absorbed by the scintillator (the other annihilation photon escapes), then the energy deposited in the detector is $T_+ + T_- + m_e = k_0 - m_e$, giving rise to another peak in the MCA spectrum m_e below the full-energy peak: thus the so-called *one-escape peak*.

Two-escape peak: If both electron-positron annihilation photons escape from the scintillator, then the only energy deposited is $T_+ + T_- = k_0 - 2m_e$, giving rise to a peak in the MCA spectrum $2m_e$ below the full-energy peak: the *two-escape peak*.

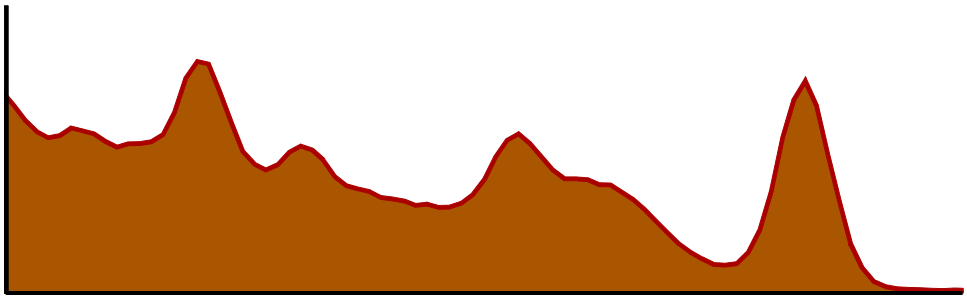

Figure 10: A portion of an MCA spectrum of ^{232}Th showing the 2.6MeV γ-ray full-energy peak (far right) and pair-production one-escape and two-escape peaks at energies $1m_e$ and $2m_e$ below it. The escape peaks sit atop the 2.6MeV γ-ray's Compton scattering spectrum. Another relatively strong full-energy peak is also apparent in the spectrum near the two-escape peak.

Of course, either annihilation photon could simply Compton scatter, depositing just a fraction of its energy in the scintillator. This event would contribute to the displayed counts between the three peaks just described.

Coincidence (sum) peaks

If the source is strong or if it is very close to the scintillator, then it is very likely that more than one γ-ray photon may enter the scintillator nearly simultaneously. The NaI scintillator has an output current pulse width of $\sim 1\,\mu$sec, so if two different photons were to interact with the scintillator within this time interval, then the energies they deposit may be combined by the MCA system into a single, large detection. For example, if both photons are photoelectrically absorbed, then to the detector this could appear to be a single "full-energy" event at the sum of the two photons' energies. These *coincidence events* can give rise to *sum peaks* in the MCA spectrum. In particular, a single nuclear decay may emit several γ-ray photons in very quick succession (refer to the ^{60}Co and ^{133}Ba decays in *APPENDIX A: Nuclear beta decay diagrams* for examples), and it may be quite likely that more than one of these photons may enter the

scintillator. Successful interpretation of the MCA spectrum from such a source will require you to consider the possibility of coincidence events and to look for sum peaks in the spectrum. In fact, the left-most strong peak in the ^{232}Th spectrum shown in Figure 10 is actually a sum peak generated by two γ-ray photons with energies of approximately 0.7–0.8 MeV.

COUNTING STATISTICS AND THE POISSON DISTRIBUTION

Examine the sample MCA spectrum in Figure 8 on page 14 again. There are two important sources of uncertainty affecting the spectrum's displayed data that depend on what are called *counting statistics*. One important effect is evident, for example, in the "fuzziness" or "noise" in the nearly flat region of the spectrum between channels 300 and 500. Another, less obvious but very important, effect of counting statistics determines the energy resolution of the MCA spectrum—in particular, the widths of the 32 keV and 0.66 MeV photon full-energy peaks. In this section we briefly explore the origins of these effects on our spectra's accuracies.

Decays of the various radioactive nuclei in a source are completely random and independent of one another, but over time intervals much shorter than the isotope's half-life, there will be an expected average decay rate: $r = n/\tau$, where n is the number of radioactive nuclei and τ is their *mean lifetime* ($\tau = \tau_{1/2}/\ln[2]$ for half-life $\tau_{1/2}$). Given the geometry of the experimental set-up, the composition of the scintillator, and the probabilities for the various interactions in it, there will be some average expected rate for detections in any one particular MCA spectrum energy channel. Those detections, however, will also be completely random and independent of one another, because the arrivals of different incoming photons are random events, and these photons will generally interact with well-separated, independent atoms of the scintillator. Statisticians call such a sequence of events a *Poisson process*[6]: events occur at times which are completely random and independent, but there is nevertheless a long-term, mean event arrival rate.

Given a Poisson process with a mean event rate r, then the expected (average) number of events μ in any finite time interval t would be $\mu = rt$. The randomness and independence of the events, however, suggest that the actual numbers of events observed during intervals of length t would vary randomly from trial to trial. These *counting statistics* are characterized by the *Poisson distribution*, described by the following probability equation:

$$P(N;\mu) = \frac{\mu^N}{N!}\, e^{-\mu} \qquad (30.5)$$

$P(N;\mu)$ is the probability of observing exactly N randomly-occurring events during a particular time interval when the expected (mean) event number during such an interval is μ. The *variance* of the Poisson distribution with expected value μ is also equal to μ, so that

[6] The eponymous mathematician Siméon Denis Poisson published his probability theory and famous distribution in 1837, although a similar result had been published in London by Abraham de Moivre over a century earlier.

***Poisson distribution standard deviation*:** $\boxed{\sigma = \sqrt{\mu}}$ (30.6)

The Poisson distribution is *discrete*, because N must be a nonnegative integer. The mean number μ, however, may be any nonnegative real number, since it represents a long-term average of the numbers N of events observed during many, many trials. Figure 11 shows plots of the Poisson distribution for various expected numbers of counts. As should be rather apparent from the figure, if the expected number μ is larger than 10 or so, we can accurately approximate the Poisson distribution by a normal (Gaussian) distribution with mean and variance both equal to μ.

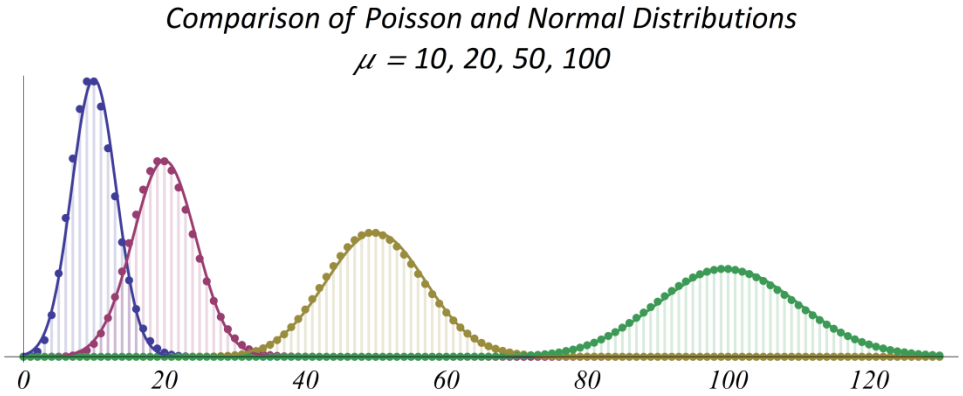

Figure 11: Plots of Poisson distribution *P*(*N*) vs. *N* for four different values of the expected number of counts μ. Also plotted for each μ is a Gaussian (Normal) distribution with variance = mean = μ.

The Poisson distributions with $\mu \leq 5$, however, are significantly different from Gaussians that have the same mean and variance. In particular, the Gaussians have significant nonzero probabilities of finding $N < 0$, which is, of course, unrealistic for an actual counting experiment.

Suppose that given a particular arrangement of a source and the detection apparatus, we expect that the average rate of accumulation of counts in a particular MCA channel to be some number r (counts/sec). After accumulating an MCA spectrum for t seconds, we would then expect that, on average, we should have $\mu = rt$ counts in that channel. The counting statistics would predict, however, that from trial to trial our observed numbers of counts N would show a variation described by the Poisson distribution, and the standard deviation of our observed numbers N around μ should be $\mu^{1/2}$. If a group of MCA channels are expected to each collect counts at about the same average rate r, then a particular spectrum should show a random distribution of counts in these various channels, again with standard deviation $\mu^{1/2}$ around the mean count μ. This fact explains the channel-to-channel "noise" displayed in the spectrum of Figure 8. If the observed fluctuations are indeed consistent with this estimate, then we say that the spectrum's uncertainty is *limited by counting statistics*; if the fluctuations are clearly greater than this value, then some other source of noise makes a significant contribution to the accuracy of the data.

The displayed widths of the full-energy peaks in the MCA spectrum of Figure 8 are also limited by counting statistics and the Poisson distribution, this time due to the poor efficiency of the

photomultiplier for detecting visible-light photons generated by the scintillator. This problem is investigated in detail in this text's *Appendix C: MCA spectrum energy resolution*. Please read that section for an explanation of the energy resolution limits of a scintillator-photomultiplier detector.

EXPERIMENT 30A

This experiment is designed to introduce you to γ-ray spectroscopy using a Sodium Iodide (NaI) scintillation detector and MCA system. Goals for this experiment:

- Become familiar with the detector and the MCA electronics.
- Understand the decay schemes in *APPENDIX A: Nuclear beta decay diagrams* of the various radioactive nuclei and the particles they emit.
- Roughly understand the physics of the interactions of high-energy photons in matter in general and in the scintillator in particular. Identify the various features in a γ-ray spectrum.
- Understand the statistical (Poisson) uncertainties associated with counting experiments.
- Be able to calibrate the MCA spectrometer and use your calibration to determine the energy of a positron annihilation photon (and thus determine the rest energy of the electron).

30a: Prelab problems

1. A nucleon is confined to a small potential well (the nucleus) with a size r of $\sim 10^{-5}$ Å . The uncertainty principle provides an estimate of the minimum momentum p ($pr = \hbar$) and kinetic energy ($2mT = p^2$) of a nucleon ($mc^2 = 940$ MeV) so confined. Provide an order of magnitude estimate of this energy (in MeV), which should give a rough scale for nuclear transitions and γ-ray energies ($\hbar c = 1970$ eVÅ).

2. Use equation (30.1) on page 6 to determine the value of $k = k_{min}$ (at $\theta = 180°$) for $k_0 \gg m_e$.

3. Derive equation (30.2) on page 6 from (30.1). The γ-ray from a ^{137}Cs decay has $k_0 = 0.66166$ MeV. Using $m_e = 0.511$ MeV, calculate the corresponding *Compton edge energy* for this photon and therefore the minimum possible energy k for its outgoing Compton-scattered photon. Do your answers agree with energies of the backscatter and Compton edge features shown in Figure 8 on page 14?

4. Refer to the *Sodium iodide mass attenuation coefficient chart* in *Appendix B: Mass attenuation coefficient charts*, page 30–B–3. What is the probability that a 0.66 MeV γ-ray emitted by ^{137}Cs travels through 5 cm of sodium iodide (NaI) ***without interacting***? Remember: $P(x) = e^{-\mu x}$. Why is it unlikely that in NaI a 1 MeV photon will undergo photoelectric absorption as its first interaction?

5. Qualitatively, how would one expect the ^{137}Cs spectrum in Figure 8 to change if the NaI scintillator were made larger? smaller? More specifically, how does the size of the scintillator affect the spectrum's "photo-fraction" (fraction of events that contribute to the full energy peak)? Sketch spectra for each case. The answer to this question lies in understanding the relative likelihood of what could happen to an outgoing Compton scattered photon before it can escape from the scintillator.

Procedure

The scintillator–photomultiplier unit is very fragile! Handle with care! Dropping the device or knocking it over will surely break it, and it costs about $2000 to replace.

The High Voltage should be set to no more than 1100 Volts unless you know what you are doing! Photomultiplier tubes can be damaged by excessive voltage.

Initial setup

Ensure that your NaI detector assembly is securely mounted to its support stand (the NaI scintillators are encased in a bare metal shield; the lab's plastic scintillator detectors are either painted blue or wrapped in black tape). Verify that the photomultiplier base (which includes the high-voltage supply and MCA electronics) is connected to the computer with a USB cable.

Start the ***Maestro*** software (there should be an icon in the task bar and on the Windows desktop). From the menu, select ***Acquire/MCB Properties*** to open the electronics properties dialog.

Initial ***MCB Properties*** dialog settings:

Amplifier tab:	**Fine Gain** 1.0; **Shaping Time** 0.75μs
ADC tab:	**Gate** Enable; **Lower Level Disc** 5; **Upper Level Disc** 1023
Stabilizer tab:	neither **Enabled** box checked
High Voltage tab:	**Target volts** 900; press the **On** button
Presets tab:	both entries blank (erased)

Leave this dialog box open for now and position it near the right edge of the display window.

Start with a ^{137}Cs source. The radioactive source material is in the small black or red end of the rod. Handle the rod by the clear plastic handle. Set the source near the detector, using hole in the top of the lead "pig" to support it.

Taking and interpreting a ^{137}Cs gamma spectrum

If the ***Maestro*** window already displays a spectrum (from a previous use), then on the ***Maestro*** window toolbar click on the ***Erase*** button (just to the right of the red ***Stop*** button). Select the toolbar's ***Log*** button to select logarithmic vertical scaling and take a spectrum by clicking on the green ***Go*** button. Click the ***Stop*** button after several seconds and you see a spectrum histogram (if nothing seems to happen, then check the ***MCB Properties*** dialog to verify that the high voltage is **ON**). With your initial gain and high-voltage settings, the ^{137}Cs 661.6 keV full energy peak should be visible somewhere in the spectrum display, although its exact location will depend on the scintillator's photomultiplier efficiency.

- Compare your spectrum to Figure 8. Use ***Erase***, ***Go***, and ***Stop*** to take new spectra. Familiarize yourself with the toolbar controls, especially the vertical scale settings: ***Log*** and ***A*** (for linear vertical *autoscale*).
- Now adjust the ***MCB Properties*** dialog's ***High Voltage*** setting, at first in increments of about 25 volts, and take new spectra. Note how the horizontal positions of the MCA spectrum features change as you change the high voltage or the ***Amplifier/Fine Gain*** settings.
- Adjust the ***High Voltage*** and ***Fine Gain*** values until the 0.6616 MeV γ-ray full-energy peak is at approximately MCA channel 768 and the 32 keV *x*-ray peak is clearly visible, as in Figure 8 (channel 1023 is at the far right edge of the display window). Take a good spectrum and save it to a file. Identify the various features in your spectrum: full energy peak, Compton distribution and edge, backscatter feature, *x*-ray peak, etc. Use Figure 8 as a guide.

Saving spectrum files for use with CurveFit, etc.

To use Maestro spectrum data with *CurveFit*, save the spectrum in ASCII SPE format, which should be the default when you open its *File Save* dialog. Load the saved spectrum file into CurveFit using the *Load Gamma spectrum* (.Spe, .tsv) file selection of the *Data I/O* menu item on the *CurveFit* palette.

Saved files can be reloaded into a Maestro spectrum *buffer* (and then resaved in other file formats if necessary). Saved spectra can be compared with a current Maestro spectrum using Maestro's *File/Compare…* menu selection.

In the lab, saved files can be plotted using Maestro's companion plotting application by double-clicking on the file icon. These plots can then be saved as PDF files using that application's *Print* menu selection and then selecting the *Microsoft Print to PDF* "printer."

- Open your saved file in *CurveFit* to check that it can be loaded successfully. Use the *CurveFit* main menu palette to navigate to the proper command to assign Poisson uncertainties to the spectrum data points (see the *Data Analysis* section for details). Next select a subrange of the data set that is dominated by the 0.66 MeV full-energy peak. Attempt a *Gaussian+Linear* fit to the data and assess the results.

If a strong noise signal is present in the very lowest channels, you can increase the ***MCB Properties/ADC/Lower Level Disc*** setting by a few channels to filter it out. How might you tell the difference between low-level noise and an *x*-ray peak with an energy of only a few 10's of keV?

Rate-Related Gain Shift

A common problem with a photomultiplier tube is that its gain may change as a function of count rate. You can check to see if your setup suffers from *rate-related gain shift* using ^{137}Cs. Place the source very close to the scintillator, take a spectrum, and estimate the channel number of the full-energy peak using the MCA cursor. Now move the source several inches back and again take a spectrum. Does the channel number of the full-energy peak shift?

If so, the following procedure seems to insure a minimum change in the photomultiplier's gain: keep the source far enough away from the detector so you can see some evidence of the *x*-ray background spectrum in your data, which rises in intensity at lower energies.

Acquiring the calibration spectra

- Roughly adjust the High Voltage and Fine Gain settings to place the ^{137}Cs γ-ray full energy peak in the lower half of the MCA spectrum.
- Now replace the source with ^{60}Co and acquire a spectrum. Readjust the settings so that both ^{60}Co full-energy peaks are fully visible near the right end of the display, leaving enough room at the high-energy end to see the 1.46 MeV ^{40}K peak you'll find when you later take a background spectrum (maybe channel 850 or so for the ^{60}Co 1.33 MeV peak).
- **Save the spectrum!** Estimate your energy calibration for the horizontal axis (keV/channel).

Leave the High Voltage and Fine Gain settings alone for the rest of the experiment! (So you don't change your calibration!)

- Take and save spectra of the various available sources (including ^{137}Cs, of course!). **Ensure that the *Lower Level Disc* is set low enough to see the *x*-rays at energies of ~30 keV.** This data will be used to perform an accurate energy calibration of the MCA channel axis. **Save all spectra for your lab analysis!** Your ^{22}Na spectrum will be used to determine the electron's mass (rest energy).
- Take a spectrum with no source (a *background* spectrum). Let the spectrum build for several minutes. Are there any recognizable full-energy peaks in the spectrum? Are there any sources being stored nearby or being used by another experimenter nearby? Do you have any ideas as to why the continuum background is more intense at lower energy? What may be causing this background activity?
- **Check the long-term stability of the system gain** by taking another ^{60}Co spectrum and compare the positions of the full energy peaks with your initial spectrum. Drift in the peak positions indicate a drift in gain, which would result in a drift in your energy calibration, a source of **systematic error**. Handle this systematic uncertainty in the calibration appropriately

when you determine the uncertainty in your electron mass determination during your data analysis.

Securing the apparatus

Turn off the high voltage before you exit the *Maestro* application. Return all sources to their containers.

Data Analysis

As was discussed in the section *Counting statistics and the Poisson distribution*, the detection of an event in any particular channel of your gamma spectra is a sample from a random process, and you would expect the number of counts in each channel to vary as you repeat the experiment. The count data in each channel is a sample from a *Poisson distribution*, which should accurately describe this variation in the counts.

For the Poisson distribution the expected variance in the counts you measure is just equal to the expected number of counts μ, so from equation (30.6) $\sigma_N = \sqrt{\mu}$ for each channel, where μ is the expected number of counts for that channel. *CurveFit* provides a function which will assign Poisson uncertainty estimates to your count data – look under ***Modify data points***: ***Transform Gamma Spectrum*** in the *CurveFit* main menu palette. The selection ***Set to Poisson count data*** will assume that the expected number of counts is well-approximated by the observed count value (y), and will assign an estimated uncertainty to each y value equal to $\sqrt{y}$ (if the count value is 0 or 1, the program will arbitrarily assign an uncertainty of 1).

- Examine a small, flat portion of a spectrum where the average count is more than about 30/channel. Estimate the channel-to-channel scatter in count number. If you assign Poisson error bars to your count data as described above and then fit that segment of the spectrum to a constant, the *reduced* χ^2 of the fit should be close to 1. Is this the case? Similarly, fitting a full-energy peak with a ***Gaussian + Linear*** function should also give a reduced χ^2 close to 1 (don't include much of the wings of the peak when doing the fit—a linear background is only an approximation).
- Plot each of your source spectra and try to identify all features you see (as in Figure 8 on page 14). Are there any features you can't identify but are clearly real? What can you identify in the ^{133}Ba spectrum? **Don't forget about the possibility of coincidence peaks** in a spectrum: see the section *Coincidence (sum) peaks*. The effect on the spectrum is to exhibit additional "full-energy" peaks at positions which correspond to the sums of pairs of photon energies. This effect creates several additional features in the ^{133}Ba spectrum.
- Use the channel positions of the various full-energy peaks to generate a calibration data set consisting of (channel number, energy) pairs and then make a plot of MCA channel number versus energy E. Do not include the ^{22}Na *positron annihilation peak* near 0.5 MeV in your calibration data set (but *do* use the ^{22}Na 1.27 MeV γ-ray full-energy peak). Try linear and quadratic fits to your data, but realize that the response of the detector system should be quite linear above 100 keV or so (away from the NaI K-edge, shown in the *Sodium iodide mass attenuation coefficient chart*). You should end up with a calibration function which converts channel number to energy (in keV or MeV). How reliable is your calibration function for energies of 100 keV or less?
- Use your calibration to determine the energy of the ^{22}Na positron annihilation peak (with uncertainty). What does this tell you about the rest energy of the electron? How does any long-

term drift is peak position (remember the two ^{60}Co spectra you acquired) affect the uncertainty in your result?

- Use your calibration and draw a vertical line on your ^{137}Cs spectrum at the channel where the Compton edge energy should occur. Does this position (should be approximately 1/3 down from the peak of the hump) correspond to the position shown in Figure 8 and in Figure 13 (on page 30–C–4)? Use your calibration to determine the energy of your ^{137}Cs spectrum's backscatter feature. Does this match your calculation from Prelab problem 3?

EXPERIMENT 30B

This experiment continues your study of γ-ray spectroscopy using scintillation detectors. You will:

- Look for *x*-ray fluorescence from a lead absorber excited by a *γ*-ray source.
- Recognize a sum (coincidence) peak in a *γ*-ray spectrum.
- Use a ^{232}Th source to see evidence of electron-positron pair production in a NaI detector. Use that spectrum to again estimate the electron rest energy.
- Use a plastic scintillator and note the differences in the detection properties between it and NaI. Fit your data using a theoretical model of a scintillator Compton spectrum.
- Understand how Poisson statistics and the scintillator-photomultiplier energy/photoelectron (E_{pe}) affects the MCA energy resolution.

30b: Prelab problems

1. Which element in the NaI scintillator is mainly responsible for photoelectric absorption? Why? The plastic scintillator you will use is composed of carbon and hydrogen. Given the *Z* dependence of σ_{photo} in equation (30.4) on page 8 and the fact that your plastic scintillator is only about 1cm thick (vs. 5cm for the NaI scintillators), how would you expect the ^{137}Cs spectrum shown in Figure 8 on page 14 to change if the detector were plastic instead of NaI? (Make a sketch). Review *Appendix B: Mass attenuation coefficient charts*.

2. What features in the ^{232}Th spectrum of Figure 10 on page 19 show that pair production is evident in the NaI scintillation detector used to acquire that spectrum?

3. For your data analysis you will use the notebook: Compton_Spectra1.nb available at:

   http://www.sophphx.caltech.edu/Physics_7/Mathematica_Notebooks/Compton%20Spectra%20Calculators/

   Download the notebook and the sample gamma spectrum file cs137_Compton_Sample.tsv Open the notebook and execute its initialization cells. Explore its features and push the **Fit Single** button on its palette. Follow the instructions, load the ^{137}Cs sample gamma spectrum file you copied, and attempt to fit its Compton spectrum. Present your fit results and a plot.

4. Review the section *Counting statistics and the Poisson distribution* on page 20. Study *Appendix C: MCA spectrum energy resolution*. Assume that an NaI MCA spectrum of the full-energy peak of ^{137}Cs (0.6616 MeV) is fit to a Gaussian: the Gaussian's mean is ADC bin $867.04 \pm .06$ and its sigma is $25.5 \pm .07$ bins. Consider equation (30.C.6) on page 30–C–2. If ADC channel number is proportional to energy, so that $\sigma(bin)/\mu(bin) = \sigma(T_e)/T_e$, then show that the scintillator's $E_{\text{pe}} \approx 570$ eV.

Procedure

If you don't remember how to set up the apparatus and use the MCA software, review the *Initial setup* section from Experiment 30a.

Lead x-ray fluorescence

Whenever high-energy photons are photoelectrically absorbed by a heavy atom, the absorbing atom is left with a hole in one of its inner atomic electron shells. Decay of a higher-level electron into the hole leads to *x*-ray emission. This *x*-ray emission will, of course, have a characteristic energy which can be used to identify the atom. A common occurrence when using lead for shielding is the generation of *x*-rays of approximately 70–90 keV (see this document's *Appendix D: Lead x-rays*).

Set up the NaI scintillator with a ^{137}Cs source so that you get a spectrum similar to that in Figure 8 on page 14. Make sure your spectrum shows a well-defined peak for the 32keV *x*-ray from the source. Put a thin (less than 3 mm) lead absorber between the source and the scintillator and take another spectrum **using a different spectrum buffer**.

Overlay the two spectra using the MCA software. You should see a marked decrease in the 32keV *x*-ray peak, but should see another, slightly higher energy peak instead. This is the lead *x*-ray fluorescence peak. Is this *x*-ray fluorescence peak generated by Compton scattering or photoelectric absorption in the lead?

Coincidence (sum) events

Reduce the MCA gain until the ^{137}Cs full-energy peak is to the left of the center channel. With the source touching the scintillator, take a spectrum for a few minutes. Do you see events at energies higher than the full-energy peak? Is there another, weak peak at high energy in the spectrum? Compare channel numbers of this peak and the ^{137}Cs full-energy peak. What is the origin of this peak? What about the other events between the two peaks?

Replace the source with ^{60}Co and adjust the HV and gain settings to put its higher (1.33 MeV) full-energy peak at about channel 450. With the source right against the scintillator, take another spectrum using the log vertical scale. Do you notice a weak peak at about 2.5 MeV? How is this peak produced? Continue to accumulate this spectrum until that peak is fairly well-defined. Save the spectrum for calibration purposes.

How should the intensity of these coincidence peaks vary as the source is moved away from the detector?

Thorium decay and pair production

Keep the HV and gain settings from the ^{60}Co work. Get the ^{232}Th source and place it and a thick (a few millimeters) lead absorber right against the NaI detector. The purpose of the lead absorber is to reduce the number of low-energy γ-rays entering the detector, keeping the counting rate sufficiently low to minimize any rate-related gain shift. Identify the 2.61 MeV Thorium full-energy peak and the one- and two-escape peaks characteristic of pair production in the scintillator. Save the spectrum for later analysis.

The plastic scintillator

Return to ^{137}Cs and reset the HV and amplifier settings to those you used for the lead *x*-ray investigation. Take a quick spectrum to make sure the Compton edge is at approximately channel 512 and adjust the settings if necessary. Take a good reference spectrum with your final settings. Save this buffer. Set the active buffer to a different buffer.

Now turn off the HV and hook up the plastic detector instead of NaI. Turn the HV back on and make sure you see pulses on the oscilloscope. Adjust the HV and gain so that the pulses peak close to 2V on the scope.

Using a different buffer from that which holds your NaI spectrum, take a spectrum using the plastic scintillator. If necessary, make fine adjustments to the gain so that the Compton edge is at the same channel as that of the NaI spectrum. Compare the two spectra. Which detector has a higher E_{pe}? Do you see any evidence of a full energy peak in the plastic scintillator spectrum? Save the spectrum and then take a ^{60}Co spectrum as well (adjust the gain so that the Compton edge is evident in the spectrum.

The sophomore lab *Mathematica* application `Compton_Spectra1.nb` may be used to attempt to fit your plastic scintillator spectra, **as long as they are of high-quality**.

Securing the apparatus

Turn off the high voltage before you exit the MCA application. Return all sources to their containers. Reconnect the NaI scintillator to the MCA electronics.

Data Analysis

Determine the energy of the lead *x*-ray fluorescence peak using the 32keV and 661.6keV ^{137}Cs peaks for an approximate, two-point energy calibration.

Use the ^{60}Co spectrum and ^{232}Th full-energy peak to calibrate your energy axis for your pair production spectrum. Use this calibration to determine the energy spacing between the ^{232}Th full-energy peak and the one- and two-escape peaks. Use these results to estimate the electron rest energy. Does the one-escape peak give as accurate a result as the two-escape peak? Why or why not?

Compare the ^{137}Cs Compton edges for the NaI and plastic scintillators. Use the mean and σ of a Gaussian+Linear fit to your NaI ^{137}Cs 661.6 keV full-energy peak to estimate the mean number of photoelectrons generated by a 661.6 keV full-energy detection. Determine the NaI detector's average *energy per photoelectron* (E_{pe}) using equation (30.C.6).

Use the Compton_Spectra1.nb application to generate a Compton spectrum similar to your plastic scintillator spectrum. What E_{pe} do you need to use to give a good match to the shapes of the spectra near the Compton edge? Note that the actual scintillator spectrum rises substantially at low energies, which implies that there are other things happening in the detector at low energy besides Compton scattering. Compare your ^{60}Co plastic scintillator spectrum to the model in Compton_Spectra1.nb.

Attempt to fit your ^{137}Cs plastic scintillator Compton spectrum using the application. Follow its instructions carefully.

APPENDIX A: NUCLEAR BETA DECAY DIAGRAMS

Cesium-137

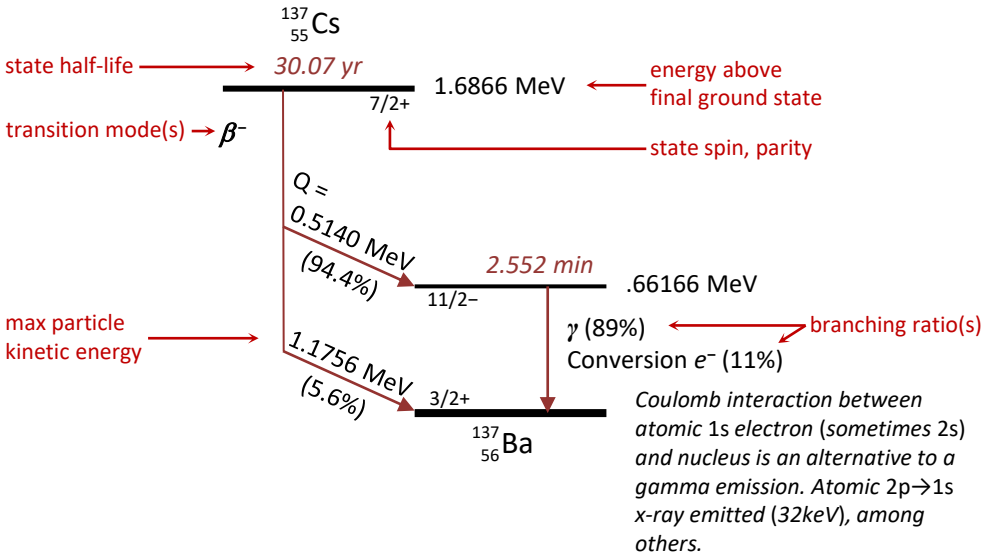

Barium-133

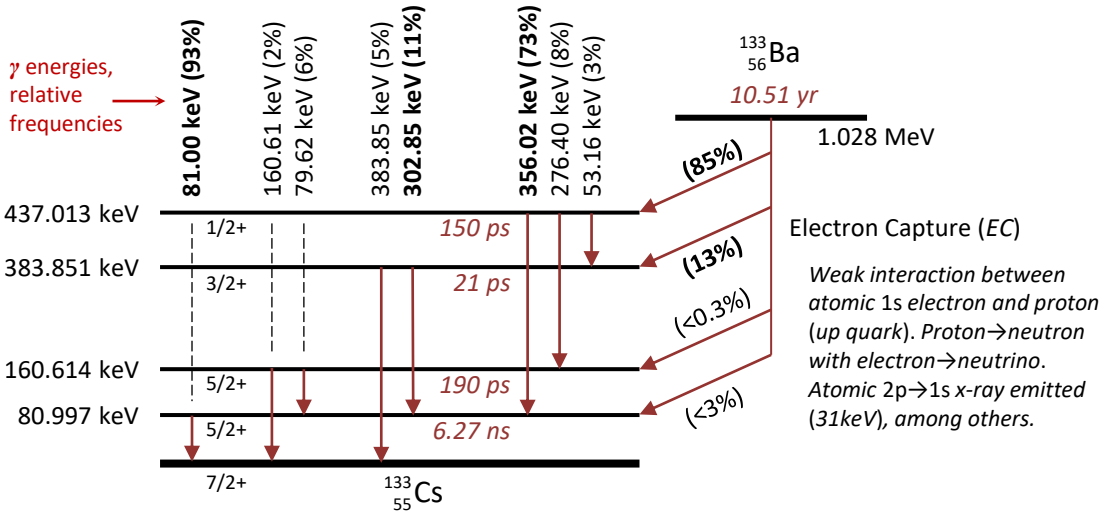

Cobalt-60

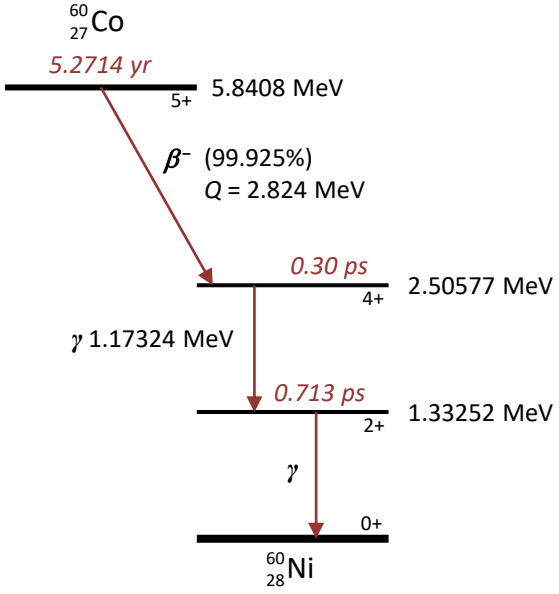

Cobalt-57

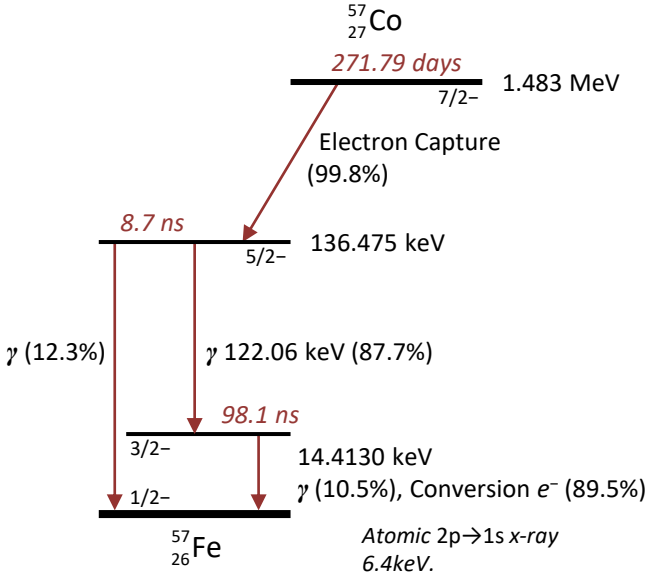

Sodium-22

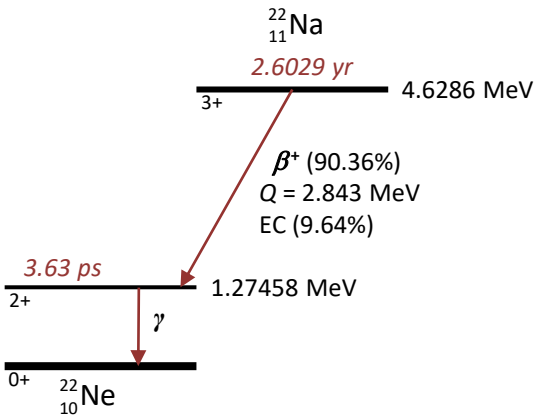

Potassium-40

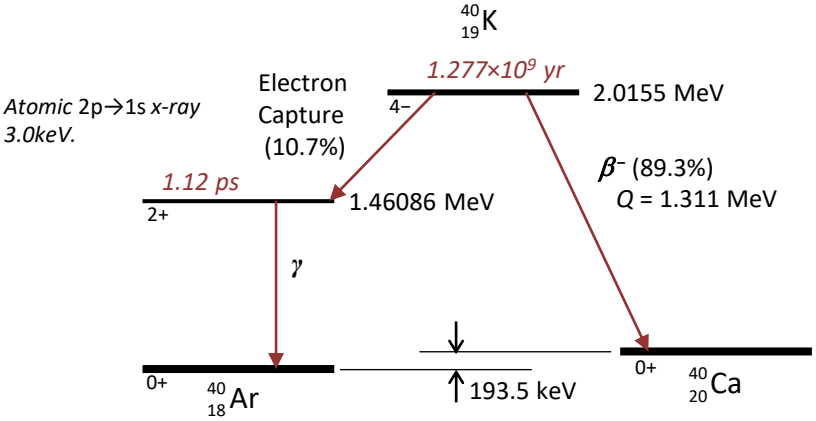

Thorium-232

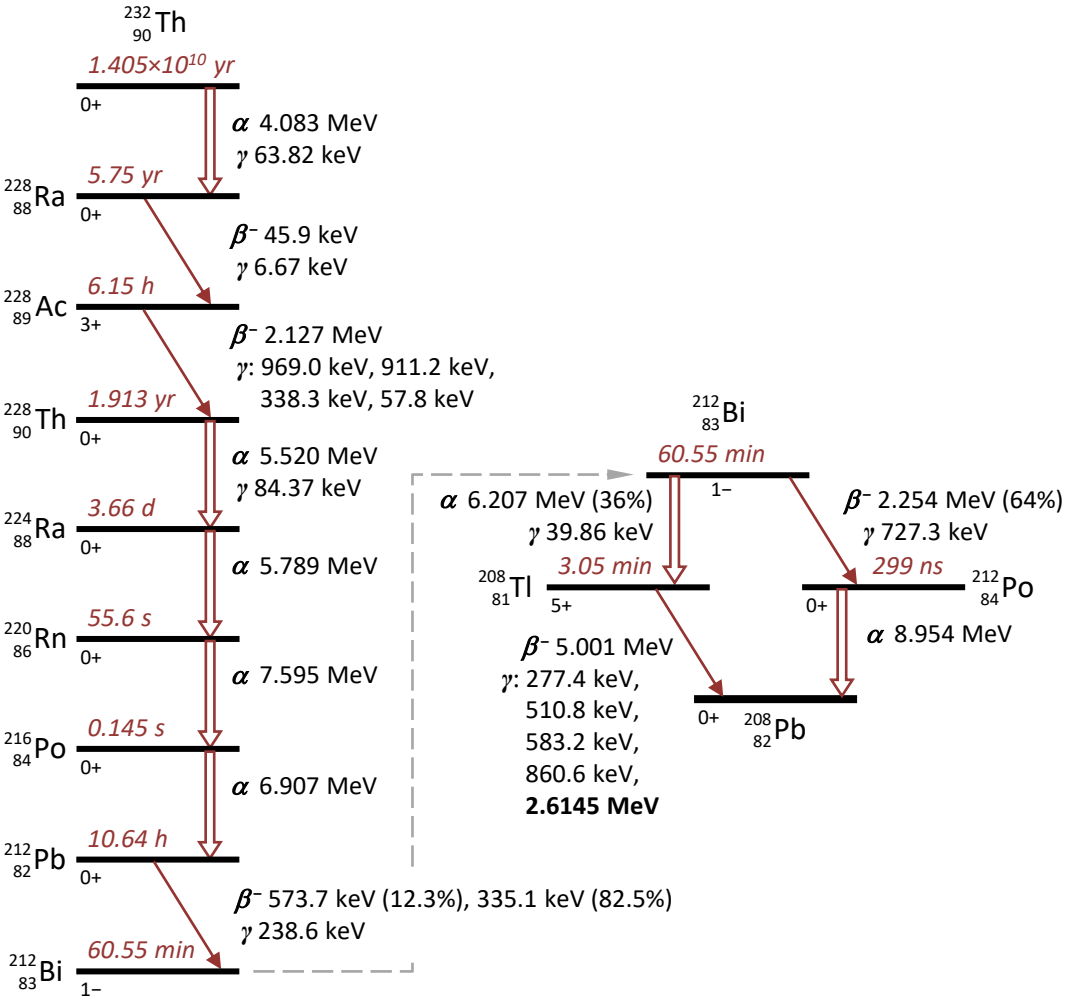

References for the decays:

Laboratoire National Henri Becquerel: Nuclear Data Table
(Gif-sur-Yvette Cedex, France)
http://www.lnhb.fr/nuclear-data/nuclear-data-table/

The Lund/LBNL Nuclear Data Search
http://nucleardata.nuclear.lu.se/toi/abouttoi.htm

APPENDIX B: MASS ATTENUATION COEFFICIENT CHARTS

As a high-energy photon passes through an assemblage of atoms, it may interact with one of them through one of the mechanisms described in the text (even if it is only Compton scattered, the outgoing photon will generally have a very different energy and direction of motion, and is clearly different from the original photon). As the photon traverses an infinitesimal thickness dx of a region containing potential targets, it has some small probability of an interaction which is proportional to dx and independent of how much material the photon has so far successfully penetrated. Therefore if the photon has probability $P(x)$ of surviving for a finite distance x through the material, then the probability it will survive to $x+dx$ is given by the differential equation

$$P(x+dx) = P(x)(1-\mu dx)$$

where μdx is that small differential probability that the photon will suffer an interaction somewhere in the next thickness dx. The solution to this equation, with initial condition $P(0)=1$, is:

***Probability to reach distance x*:** $\boxed{P(x) = e^{-\mu x}}$ (30.B.1)

where the *absorption coefficient* μ is determined by the characteristics of the material and the energy of the photon and has units of (length)$^{-1}$. The expected fraction of a beam of photons to emerge after passing through a thickness x of a material is just given by the probability expression (30.B.1). The photon's *mean free path* λ is given by $\lambda = 1/\mu$ and is the mean distance through the material traveled by a typical photon before suffering an interaction. To follow the rest of this brief discussion about μ, *cross sections*, and the *mass attenuation coefficient* please read through General Appendix B: Cross Sections.

Since the Compton scattering, photoelectric absorption, and pair production interactions of a photon with an atom are independent and mutually exclusive, the *total interaction cross section* for the photon and atom is given by the sum of the individual Compton, photoelectric and pair production cross sections:

$$\sigma_{\text{total}} = \sigma_{\text{Compton}} + \sigma_{\text{photo}} + \sigma_{\text{pair}}$$

In terms of the total cross section σ_{total} for interaction with a single atom, the absorption coefficient μ is given by (General Appendix B, equations B-13 through B-16):

$$\mu = n\,\sigma_{\text{total}} = \frac{\rho N_A}{A}\sigma_{\text{total}}$$

where n is the number density of the atoms, ρ is their mass density, A is the molar mass of the material, and N_A is Avogadro's number.

The absorption efficiency of a material is normally presented as a *mass attenuation coefficient* (μ/ρ), rather than its absorption coefficient μ. Thus the value of the mass attenuation coefficient must be multiplied by the material's mass density to calculate μ for use in equation (30.B.1).

Mass Attenuation Coefficient **= μ/ρ and has units (length)^2/mass.**

The graphs on the next several pages display the contributions to the mass attenuation coefficient as a function of photon energy for several important materials. These charts were constructed from data supplied by the

XCOM: Photon Cross Sections Database
available at the NIST website: http://www.nist.gov/pml/data/xcom/.

Three remarks about the graphs:

a) The difference between the Klein-Nishina cross section (Figure 3 on page 7) and the *Compton* data in the graphs: the Klein-Nishina cross section describes Compton scattering by *a single free electron*, whereas the Compton contribution in a mass attenuation graph is due to scattering by all of an atom's electrons. The actual total atomic Compton cross section decreases at low photon energies because tightly bound electrons do not contribute as much to the Compton process (Why? Hint: what is the "effective" mass of an electron tightly bound to the much heavier nucleus? How should this mass affect the cross section?)

b) The rapid decrease of the photoelectric coefficient with increasing photon energy is due to the resonant nature of photoelectric absorption and is readily apparent in the figures. Various *K*-edges are also evident, corresponding to the binding energy of the *K* shell (1s) electrons.

c) The mass attenuation coefficients μ/ρ in the figures are for single interactions in the material, which is the case only when the size of the material is small. For example, if the material is large (with dimensions comparable to or greater than the mean free path λ), then the probability of another event involving the outgoing photon from an initial Compton scattering event may be quite significant, and the total energy absorbed by the material is increased over what would be expected from just a single event. The consequences of this effect were considered in the text's discussion of the expected scintillation spectra. *The details of observed spectra can only be understood when multiple events are considered*.

Remember that the mass attenuation figures from the following graphs must be multiplied by the density of the material to determine the absorption coefficient μ and the mean free path $\lambda = 1/\mu$.

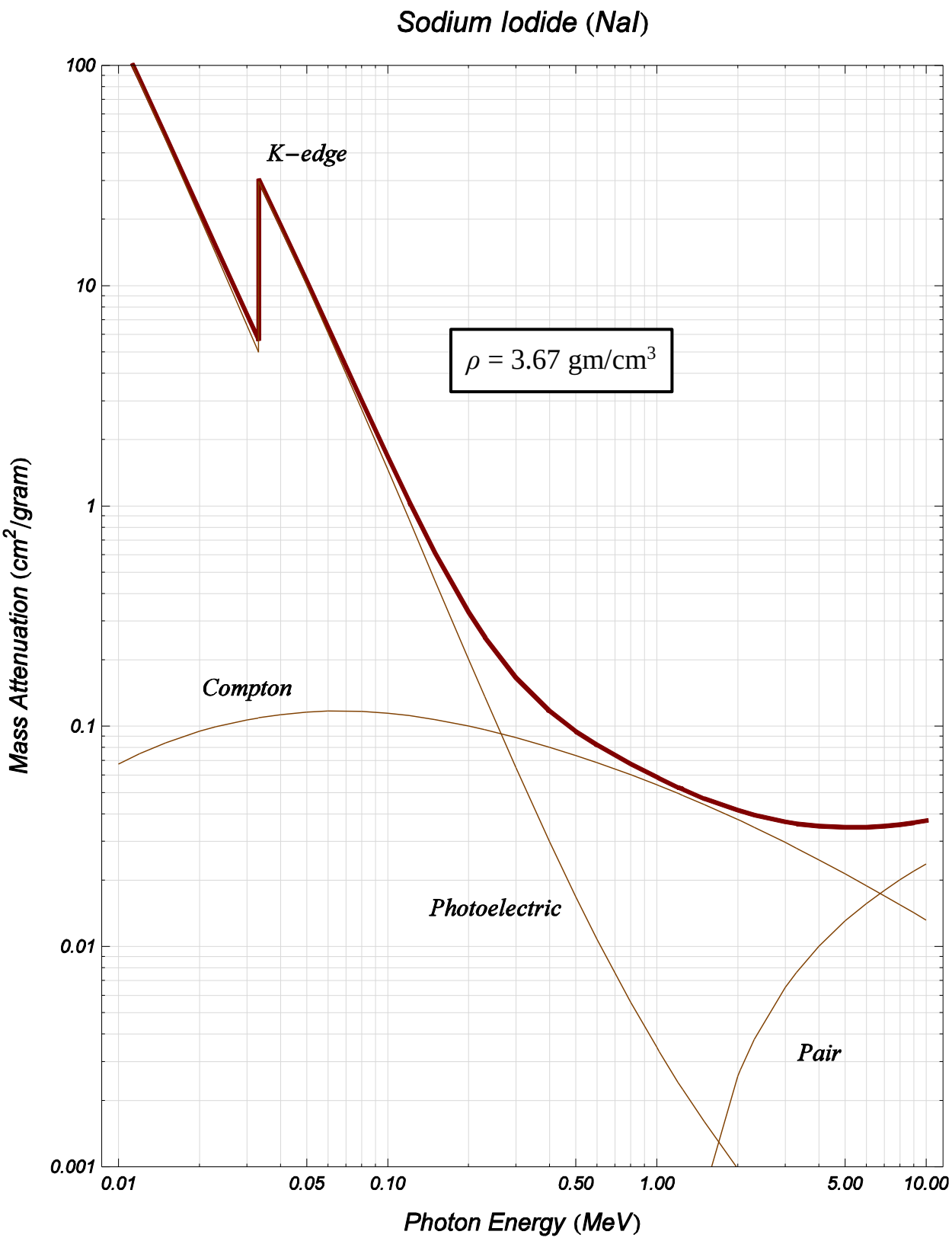
Sodium Iodide (NaI)
100
10
1
0.1
0.01
0.001
K−edge
ρ = 3.67 gm/cm3
Compton
Photoelectric
Pair
Mass Attenuation (cm2/gram)
0.01
0.05
0.10
0.50
1.00
5.00
10.00
Photon Energy (MeV)

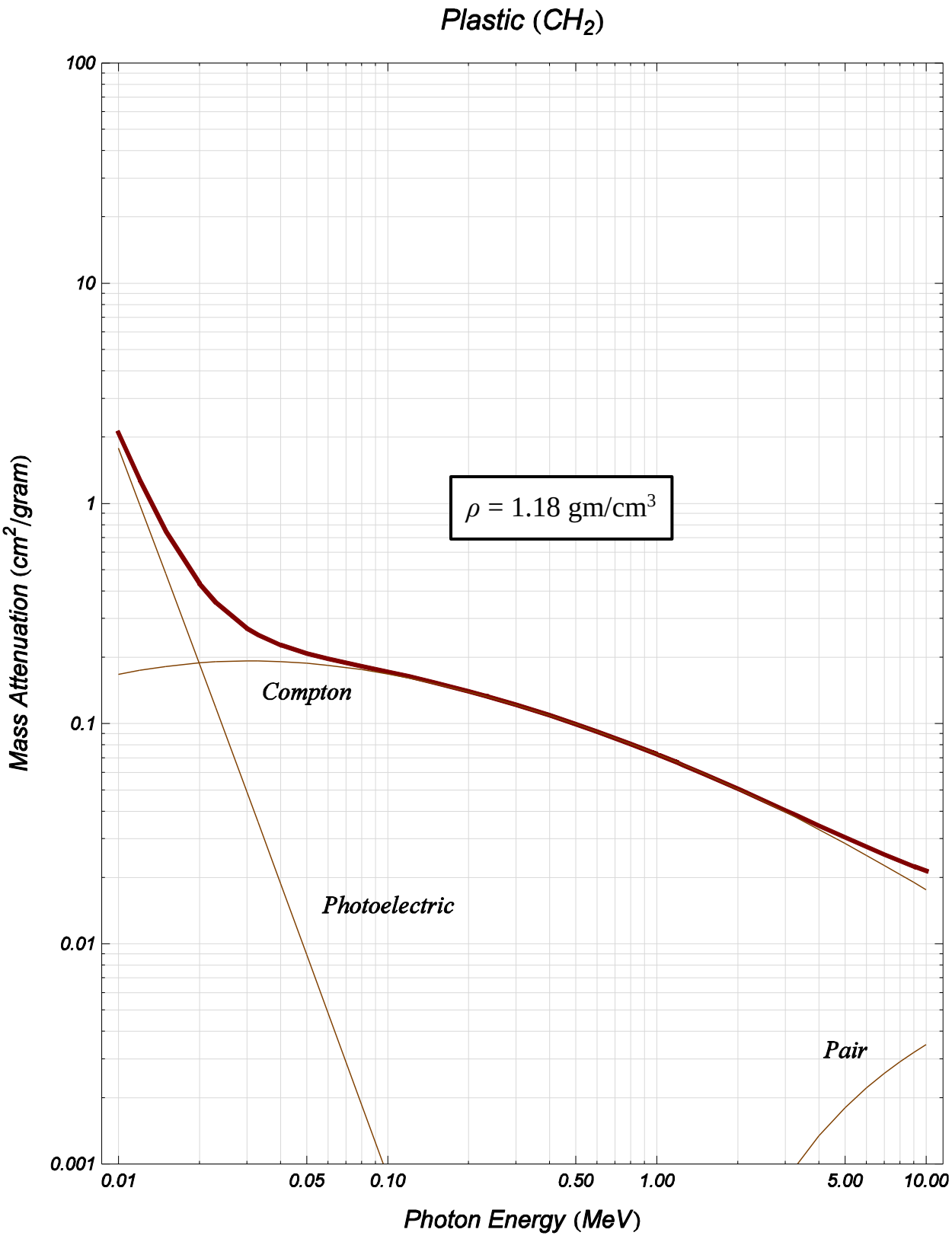
Plastic (CH_2)
100
10
1
0.1
0.01
0.001
Mass Attenuation (cm^2/gram)
ρ = 1.18 gm/cm^3
Compton
Photoelectric
Pair
0.01
0.05
0.10
0.50
1.00
5.00
10.00
Photon Energy (MeV)

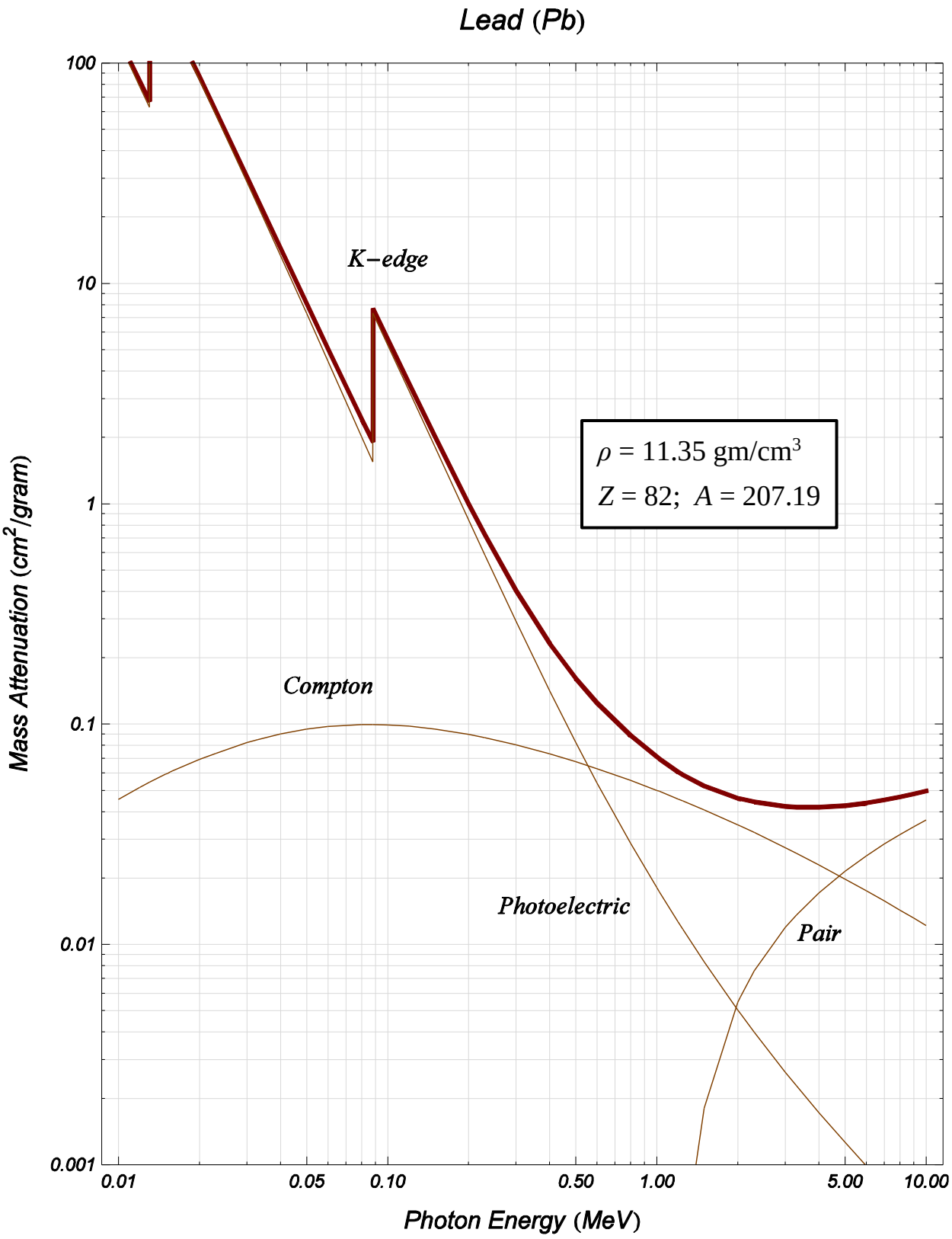
Lead (Pb)
100
10
1
0.1
0.01
0.001
Mass Attenuation (cm²/gram)
K−edge
Compton
Photoelectric
Pair
ρ = 11.35 gm/cm³
Z = 82; A = 207.19
0.01
0.05
0.10
0.50
1.00
5.00
10.00
Photon Energy (MeV)

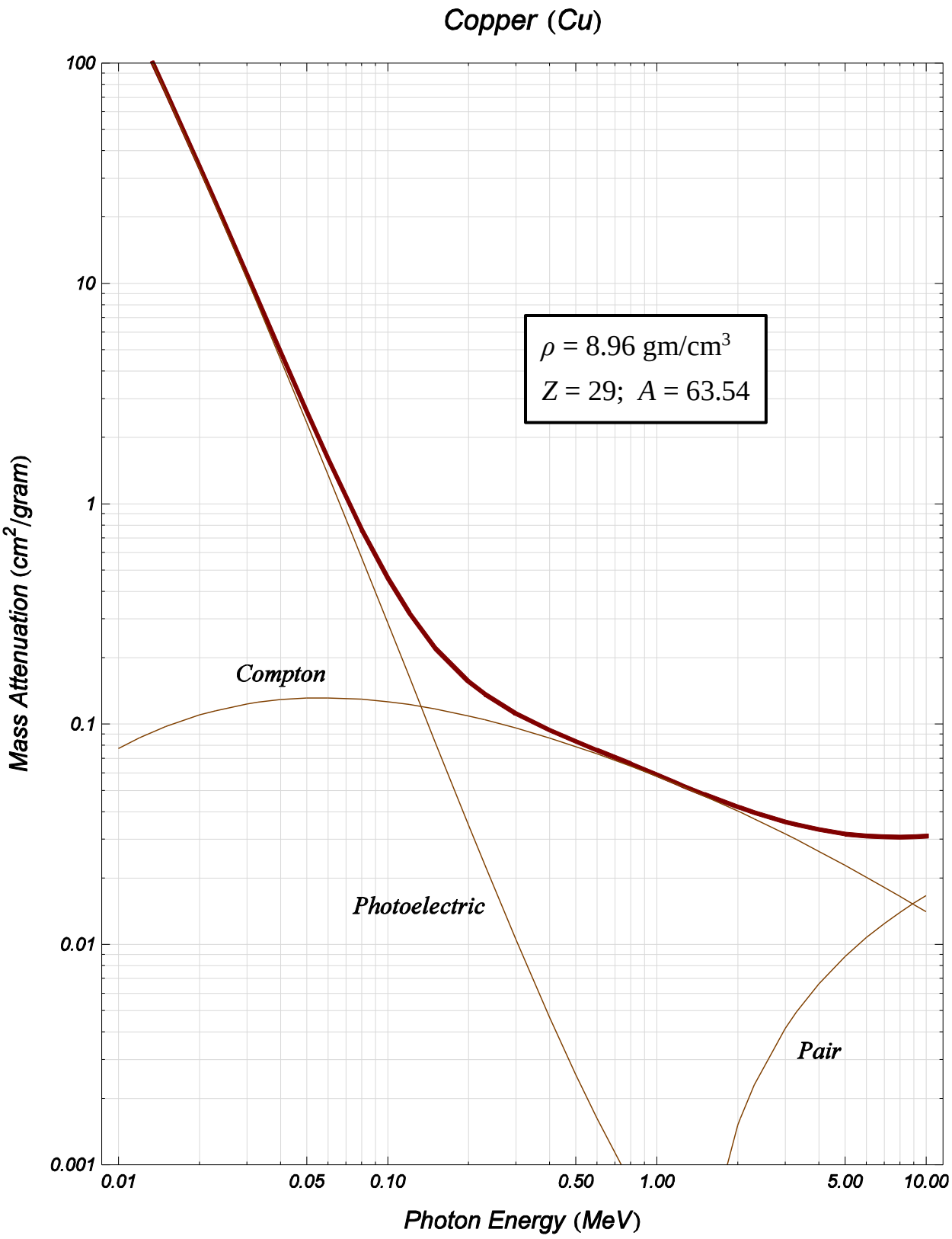
Copper (Cu)
100
10
1
0.1
0.01
0.001
Mass Attenuation (cm²/gram)
ρ = 8.96 gm/cm³
Z = 29; A = 63.54
Compton
Photoelectric
Pair
0.01
0.05
0.10
0.50
1.00
5.00
10.00
Photon Energy (MeV)

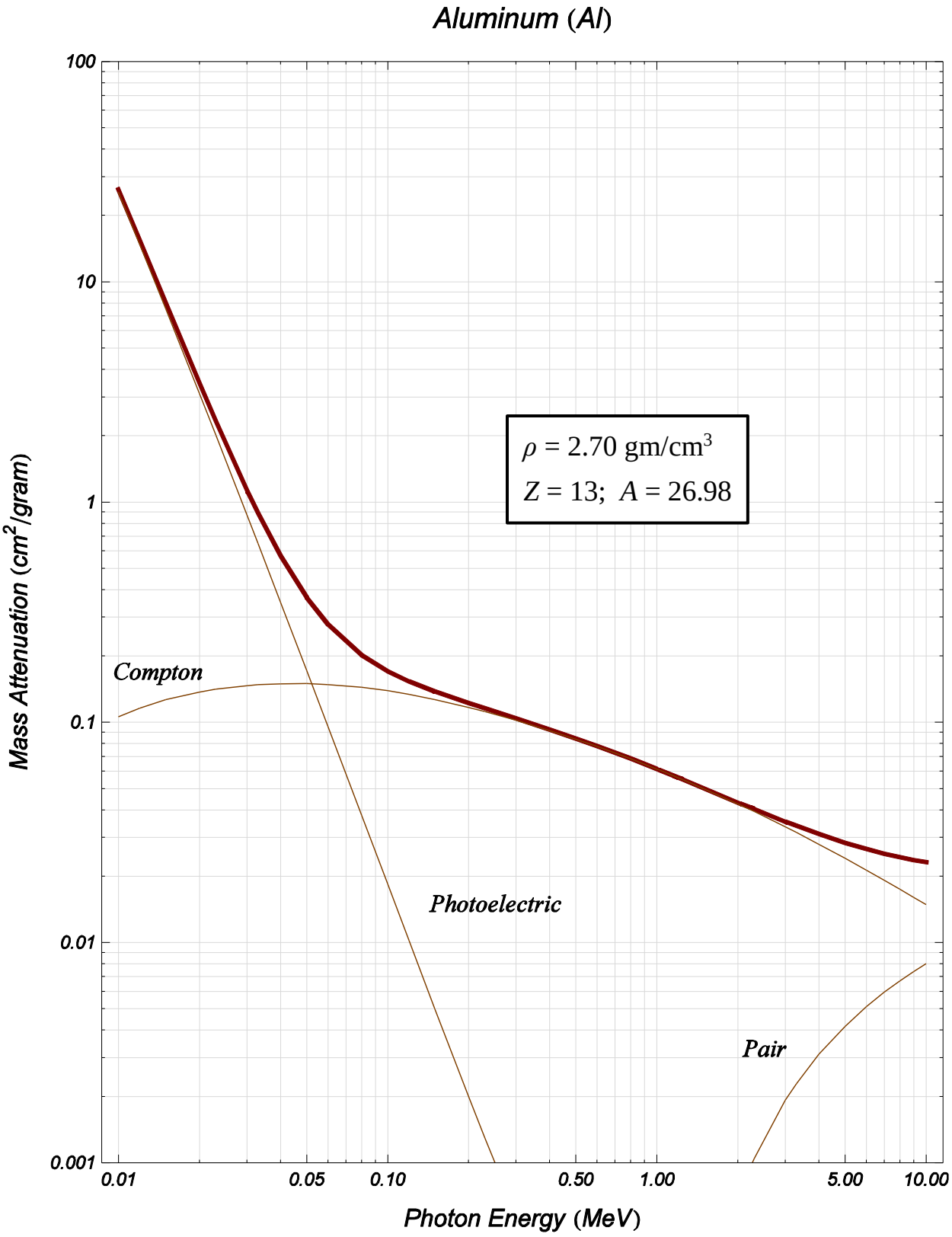
Aluminum (Al)
100
10
1
0.1
0.01
0.001
Mass Attenuation (cm²/gram)
ρ = 2.70 gm/cm³
Z = 13; A = 26.98
Compton
Photoelectric
Pair
0.01
0.05
0.10
0.50
1.00
5.00
10.00
Photon Energy (MeV)

APPENDIX C: MCA SPECTRUM ENERGY RESOLUTION

Due to statistical fluctuations the one-to-one relation between energy deposited in the scintillator and the final displayed MCA channel number for an event is only true on average. Notice the width of the 0.66 MeV full-energy peak displayed in the MCA spectrum shown in Figure 8 on page 14. This width is due to the statistical nature of the conversion of energy in the scintillator to the number of electrons at the photomultiplier output, and the resultant variation in that output given a fixed energy deposited by an incident photon. The most important source of this variation is the finite probability that a photon striking the photomultiplier's photocathode will actually release an electron: ***only a small fraction of the available optical photons actually generate photoelectrons.*** A scintillator-photomultiplier system can be characterized by the average energy deposited in the scintillator necessary to produce one photoelectron: E_{pe}.

$$E_{\text{pe}} \equiv \text{mean energy/photoelectron (eV)}$$

For the NaI scintillators used in the lab E_{pe} ranges from 600 to 1200 eV; for a plastic scintillator the conversion is generally much less efficient. The expected (mean) number of photoelectrons μ corresponding to an energy T_e deposited in the scintillator is thus given by:

$$\mu = \frac{T_e}{E_{\text{pe}}} \tag{30.C.1}$$

Let's calculate a typical μ. For $T_e = 1\,\text{MeV}$ and $E_{\text{pe}} = 700$ eV, $\mu = \dfrac{1\,\text{MeV}}{700\,\text{eV}} \approx 1400$

The μ calculated above is an average; the actual number of photoelectrons generated by any particular event will vary about this value. The Poisson distribution of equation (30.5) also provides the statistics which describe this fluctuation in the number, because the system counts *random*, *independent events*: each individual optical photon may or may not generate a photoelectron, and the optical photons associated with a particular event are actually independent, since they were each generated by different, independent electron-ion recombinations in the scintillator. As the section *Counting statistics and the Poisson distribution* describes, the expected variation in the number of photoelectrons around the average μ is then given by:

***Poisson distribution standard deviation*:** $\boxed{\sigma_N = \sqrt{\mu}\,; \quad \therefore \frac{\sigma_N}{\mu} = \frac{1}{\sqrt{\mu}}}$ (30.C.2)

Refer back to Figure 11 on page 21 and note that the width of a peak grows as its mean μ increases, but more slowly. Also shown in that figure is how well a Gaussian distribution with the same mean and variance matches the shape of the Poisson distribution. The Gaussian probability density function for mean = variance = μ is given by (30.C.3).

$$p(N;\mu,\mu) \;=\; \frac{1}{\sqrt{2\pi\mu}}\,\exp\!\left[\frac{(N-\mu)^2}{2\mu}\right] \qquad (30.C.4)$$

This approximation of the Poisson distribution $P(N;\mu) = p(N;\mu,\mu)$ by a Gaussian is quite good for $\mu > 10$ or so. Armed with the Poisson distribution and its Gaussian approximation, we are now in a position to understand the actual shapes and widths of the MCA energy spectrum features shown in Figure 8 on page 14.

We can transform the Poisson probability distribution $P(N;\mu)$ for the *number of photoelectrons* generated by a detection (equation (30.5)) into an expression relating the MCA displayed vs. actual *deposited energies*: we do this using the energy/photoelectron E_{pe} and equation (30.C.1). This will yield the probability distribution $P(T;T_e)$, giving the probability of displaying an event at energy $T = N \times E_{\text{pe}}$ when the actual energy deposited in the scintillator was T_e (so that $\mu = T_e / E_{\text{pe}}$).

For our analysis we want to let the energies T and T_e vary continuously, whereas $P(N;\mu)$ and thus $P(T;T_e)$ is discrete (only nonnegative integer values allowed for the photoelectron count N). Consequently we replace the actual Poisson distribution with our Gaussian (30.C.4).

The Gaussian distribution in (30.C.4) with mean and variance both equal to μ gives a *probability density* $p(N;\mu,\mu)$: $p(N;\mu,\mu)dn$ gives the differential probability that the continuous variable n lies close to N. We now express this Gaussian approximation to the photoelectron distribution not in terms of the number of photoelectrons but in terms of the displayed energy T vs. the deposited energy T_e,

$$R(T;T_e) \;=\; \frac{1}{\sigma(T_e)\sqrt{2\pi}}\,\exp\!\left[-\frac{(T-T_e)^2}{2\sigma^2(T_e)}\right] \qquad (30.C.5)$$

where T_e is now the mean of the Gaussian distribution and $\sigma(T_e)$ is its yet-to-be-determined standard deviation (in terms of energy). Such a probability density $R(T;T_e)$ is often called a *response function* or *point spread function* of a measurement system and in our case determines the MCA's energy resolution. The standard deviation of the distribution around T_e, i.e. $\sigma(T_e)$, may be determined from (30.C.4) using the scintillator system's E_{pe}: $\mu = T_e / E_{\text{pe}}$

$$\frac{\sigma(T_e)}{T_e} \;=\; \frac{\sigma_N}{\mu} \;=\; \frac{1}{\sqrt{\mu}} \;=\; \sqrt{\frac{E_{\text{pe}}}{T_e}}$$

MCA Peak width vs. E_{pe}: $\boxed{\sigma(T_e) = \sqrt{T_e \times E_{\text{pe}}}\;;\quad E_{\text{pe}} = \sigma^2(T_e)/T_e}$ (30.C.6)

This expression relates the mean and standard deviation of a Gaussian fit to, for example, a full-energy peak at energy T_e to the system's E_{pe}. More generally, if an energy T_e is deposited in the

scintillator, the differential probability for the MCA system to display an energy between T and $T+dT$ is given by $R(T;T_e)dT$ using the response function in (30.C.5) with $\sigma(T_e)$ given by (30.C.6). As already mentioned, $R(T;T_e)$ therefore gives the displayed spectrum of a "monochromatic" source depositing exactly energy T_e.

If an interaction event could result in some value from a continuous distribution of energy being deposited in the scintillator with probability density $D(T_e)$ (as is the case for Compton scattering of photons in a scintillator), then the displayed energy spectrum of a large number of such events is given by a generalized sort of *convolution* of $R(T;T_e)$ and $D(T_e)$, equation (30.C.7). This convolution process is illustrated in Figure 12.

$$S(T) \;=\; R * D \;\equiv\; \int_0^\infty R(T;T_e)\,D(T_e)\,dT_e \qquad (30.C.7)$$

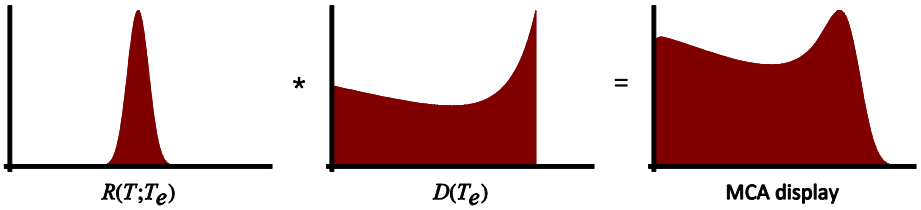

Figure 12: Displayed Compton scattering spectrum in a scintillator system with finite energy resolution. This figure graphically illustrates the "convolution" of the system's response function $R(T;T_e)$ with the actual interaction energy spectrum $D(T_e)$ using equation (30.C.7).

This convolution process in the case of a displayed Compton spectrum is described in more detail in General Appendix D: Calculating Scintillator Compton Spectra. You can explore the subject in more detail using the sophomore lab Mathematica notebook Compton_Spectra1.nb downloadable at:

http://www.sophphx.caltech.edu/Physics_7/Mathematica_Notebooks/Compton%20Spectra%20Calculators/

An example of the application's output is shown in Figure 13 (next page).

Note that the Compton edge energy corresponds to that point where the displayed spectrum is at approximately 2/3 of its maximum (the actual ratio is shown in the text above the plot in Figure 13); this is an excellent rule of thumb method to estimate the MCA channel number corresponding to a known Compton edge energy when calibrating an MCA system.

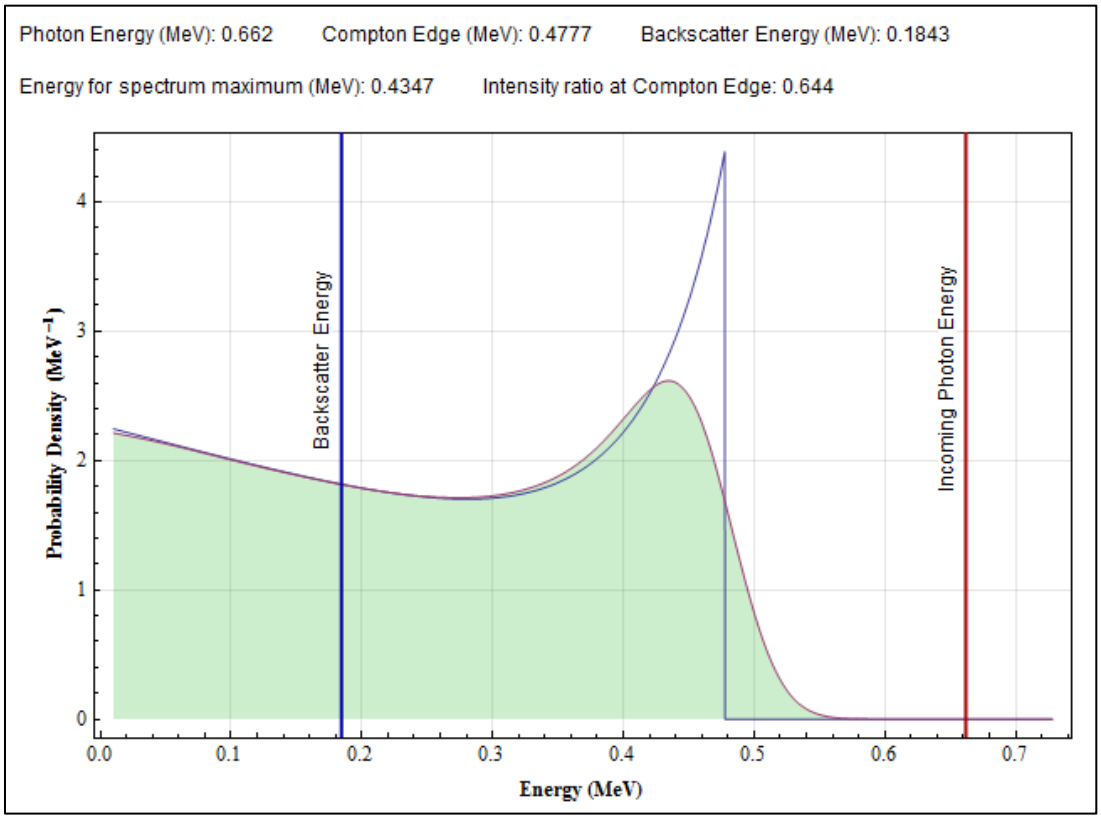

Figure 13: The Compton spectrum for a 0.662 MeV γ-ray generated using the sophomore lab "Compton_Spectra1.nb" application for *Mathematica*. The shaded curve is the displayed spectrum smoothed by the system's finite energy resolution, in this case with E_{pe} = 2keV, typical of a plastic scintillator as used in Experiment 30b. Also shown is the theoretical Compton spectrum without smoothing (the Compton edge energy T_{edge} is the abrupt cutoff at 0.478 MeV), along with vertical lines at the incoming photon energy k_0 and at the *backscatter energy*, which is the outgoing photon energy following a 180° scatter.

APPENDIX D: LEAD X-RAYS

X ray	Energy
$K_{\alpha 2}$	72.8042
$K_{\alpha 1}$	74.9694
$K_{\beta 3}$	84.45
$K_{\beta 1}$	84.936
$K_{\beta 2}^{II}$	87.23
$K_{\beta 2}^{I}$	87.364
L_{l}	9.1845
L_{η}	11.3493
$L_{\alpha 2}$	10.4495
$L_{\alpha 1}$	10.5515
$L_{\beta 1}$	12.6137
$L_{\beta 4}$	12.306
$L_{\beta 3}$	12.7933
$L_{\beta 2}$	12.6226
$L_{\gamma 1}$	14.7644

Level and transition diagram is on next page.

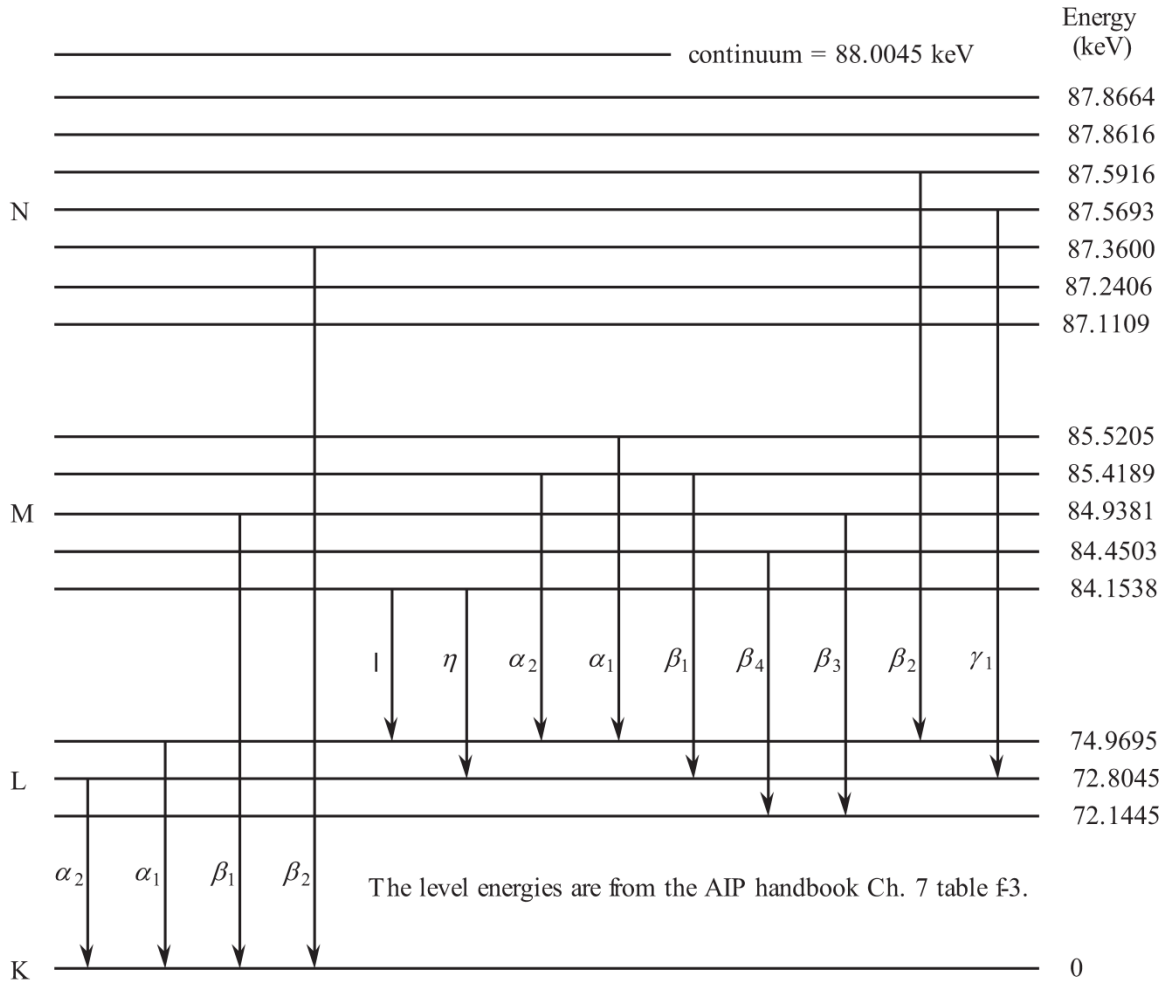
Energy
(keV)
continuum = 88.0045 keV
87.8664
87.8616
87.5916
N
87.5693
87.3600
87.2406
87.1109
85.5205
85.4189
M
84.9381
84.4503
84.1538
l
η
α2
α1
β1
β4
β3
β2
γ1
74.9695
L
72.8045
72.1445
α2
α1
β1
β2
The level energies are from the AIP handbook Ch. 7 table f-3.
K
0